Reviews for Atmos. Chem. Phys. Discuss., doi:10.5194/acp-2015-969, 2016.

Ickes Luisa[1*], Welti André[1+], and Lohmann Ulrike[1]

[1]IAC, ETH Zurich
[*]now at: IMK-AAF, KIT Karlsruhe
[+]now at: TROPOS Leipzig

Correspondence to: Luisa Ickes (luisa.ickes@env.ethz.ch)

We thank both anonymous reviewers and P. A. Alpert for their positive review and the detailed comments on the manuscript. We have revised the manuscript accordingly (see track-changes in the manuscript). Our replies to your comments are given below in blue after the specific comment.

1 Review 1

1.1 General comment:

In order to find an appropriate (CNT-based) parameterization for immersion freezing (induced by mineral dusts) in GCMs, the authors tested various combinations of different descriptions for interfacial free energy σ_{w}, activation energy $\Delta g^{\#}$ as well as different possibilities to include contact angle (single contact angle, contact angle distribution and temperature dependent contact angle). To do so, the different schemes are fitted against laboratory heterogeneous freezing data for different dusts (spanning several temperature, particle surface and time ranges).

I have to admit that after first reading I have been in two minds about recommending this paper for publication in ACP. On the one hand the authors e.g. vividly demonstrate that contact angle values gained for one substance largely depend on the values/parametrizations used for σ_{w} and $\Delta g^{\#}$ so that contact angle values obtained in different studies for a given substance do not necessarily agree. This is important if these contact angle values are used in GCMs but connected with other σ_{w} and $\Delta g^{\#}$ values/parameterizations. On the other hand e.g. I doubt the physics behind some of the presented parameterization schemes (see specific comments). However, due to the importance for the heterogeneous ice nucleation community I would recommend this paper for publication after the following comments have been addressed.

We attempt to clarify the physics behind some of the presented parameterization schemes below. However, the microphysical details how freezing of supercooled water is triggered heterogeneously are not very well understood so that some approaches are based on speculative assumptions. It is not the aim of this article to judge how reasonable the assumptions are, but to show different strategies to handle heterogeneous freezing with CNT based parametrisations and to investigate how well these parameterizations describe a selection of laboratory data.

1.2 Specific comments:

Page 1, line 10-11: I do not understand the meaning of the sentence starting with “We show that additional...”. Please clarify. What is “J_{imm}“?

We changed that in the manuscript. We also added an explanation for J_{imm}.

Page 4, line 12-13: I agree that in case of heterogeneous ice nucleation the freezing curve is shifted to higher T compared to the homogeneous case. But does the curve necessarily has to be less steep? Looking on Fig. A3 in the paper of Hoose and Möhler (2012) it can be seen that the heterogeneous nucleation rate is steeper for higher temperatures (depending on the parameterizations used in CNT). So what causes the heterogeneous freezing curve to be less step compared to the homogeneous case?

The temperature dependence of the nucleation rate J_{imm} (or J_{hom}) is controlled by the temperature dependence of the Gibbs free energy barrier ΔG and the activation energy barrier $\Delta g^{\#}$, which have opposite temperature dependences. In the case of immersion freezing ΔG is reduced and therefore the contribution of $\Delta g^{\#}$ is more important, which leads to a flattening of the heterogeneous nucleation curve compared to homogeneous nucleation. Looking at measurements of the frozen fraction as a function of T (homogeneous freezing compared to immersion freezing) one can see that indeed the curves for immersion freezing are less steep compared to homogeneous freezing.

Evaluating the steepness of different curves relative to each other is also a matter of perspective. Looking at the figure below it can be seen that when comparing the curves within the red box, the steepness increases with decreasing f (hom. freezing vs. het. freezing). Looking at the curves within the same temperature range (blue box), however, the steepness of the curve decreases in case of heterogeneous freezing. The second case is the situation we were refering to. We added a better explanation in the manuscript.

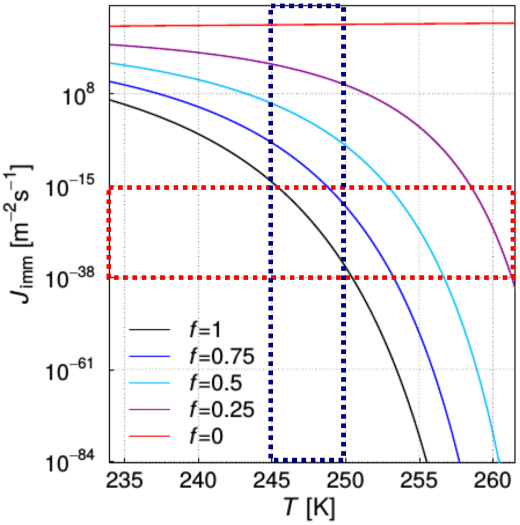

Chapter 2.1.3: I have a problem with the interpretation of the temperature dependent contact angle scheme. In a physical sense the contact angle is "determined by the condition of mechanical equilibrium, i.e., there must be no net force component along the solid surface" (Pruppacher and Klett, 1997, P. 136). Due to the decrease of the interfacial free energies with temperature does the contact angle then should decrease with decreasing temperature for a given particle (let's assume homogeneous surface conditions)? Here, the contact angle increases with decreasing T. I would interpret this behavior in that way that particles with larger contact angles (higher energy barrier) can be activated with decreasing temperature. Is this in agreement to your description?

Yes, this is in agreement. The α(T) scheme accounts for the change of the contact angles being activated at different T resulting in a shift of the contact angle distribution towards larger average contact angle with supercooling. The lower the temperature, the higher the chance that particles with larger contact angles can be activated. We clarified that in the text.

Chapter 3.1: I have some trouble with those schemes fitting $\Delta g^{\#}$. In lines 27 to 30 you mention that an aerosol type specific $\Delta g^{\#}$ value is physically questionable. On the other hand this statement is reversed on the next page saying that the particle itself might influence the diffusion of water molecules to the ice cluster. I agree that the attachment of water molecules to the ice cluster is influenced due to the presence of the ice nucleating particle i.e., the INP "blocks" water molecules since the ice cluster is just a cap and not spherical (in terms of CNT) as for the homogeneous case. But I think that n_s in CNT takes care of this. Are there any mechanisms which could confirm your hypothesis of aerosol-type specific $\Delta g^{\#}$? Is there a specific term in CNT which would take care of this? Or does $\Delta g^{\#}$ represent here just a fitting parameter without physical meaning?

n_s is the number of water molecules in contact with the unit area of an ice germ and is mostly estimated based on the molecular density of water. The activation energy $\Delta g^{\#}$ describes the diffusion of a water molecule across the water-ice boundary. Most authors assume that this diffusion process for immersion freezing is equivalent to the one for homogeneous freezing. In case of heterogeneous freezing the diffusion could be disturbed by the presence of IN in the water (surface charges, polarizability of the particle surface, etc.). Our hypothesis is that the activation energy $\Delta g^{\#}$ is different within a pure supercooled water droplet compared to a supercooled water droplet containing an insoluble aerosol particle (IN), because the IN (eventually containing surface charges) effects the hydrogen bond network and due to that could influence the diffusion process. One example study looking at the influence of surface charge on ice nucleation is the study of Edwards and Evans (1962). We added this reference.

On page 8, line 19-20 you mention that a single contact angle is not able to represent the experimental results for mineral dust. This has also been shown in e.g. Lüönd et al. (2010), Welti et al. (2012), etc. But is this a general finding? What about other substances like biological particles?

We only investigated the behavior of a single contact angle to describe heterogeneous freezing of mineral dust. We did not look at biological particles, therefore we can not make a general statement about the ability of a single contact angle to parameterize their freezing. Also ice nucleation by AgI seems to be captured by a single alpha. Possibly a single alpha scheme can be used for highly efficient IN triggering ice formation at low supercooling.

Page 9, line 18-20: I do not understand why this procedure has been performed. Some further explanations here would be great.

This exercise was done to exemplary show the consequence of using fit parameters together with a CNT formulation, which was not the one used to derive the fit parameters. We included an additional explanation to make this clearer.

Page 10, line 26-27: The curve in Fig. 4a does not approach -100%...

We only show the part of the curve where changes are large. The plot with an increased range is added below.

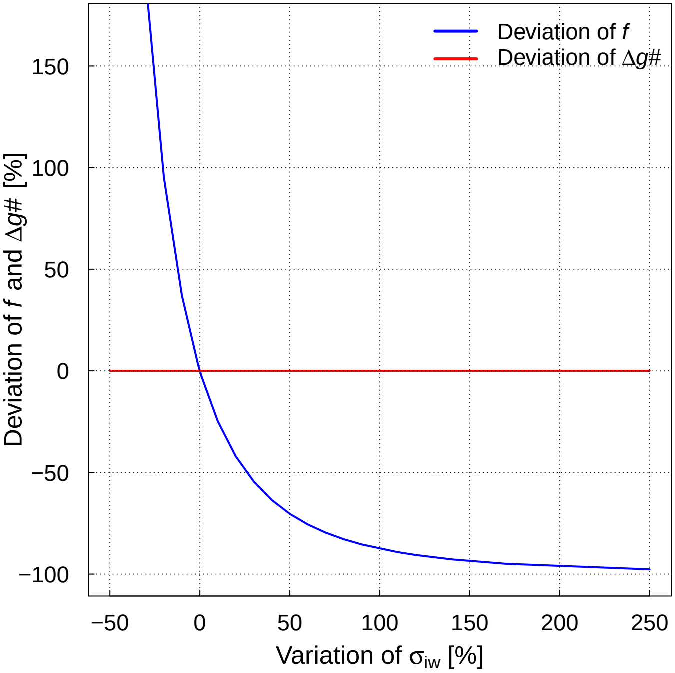

Page 10, line 30: It looks like that the compensation in Fig. 4b is not completely linear.

Thanks for recognizing this, we did not see that at the first glance. While the deviation of μ with variation of $\Delta g^{\#}$ is linear, the deviation of σ is linear for a small variation of $\Delta g^{\#}$ (until 30% approximately), but is nonlinear for larger variations of $\Delta g^{\#}$. We adapted the text accordingly.

Chapter 6 and Appendix C (especially Fig. 9), concerning particle size dependence: Do you know the reason for the change of the contact angle distribution with particle size for the kaolinite sample? In general, does the ice nucleation ability of a given substance has to scale with particle size? How pure is the used kaolinite sample as well as the other samples and is it possible that the chemical composition of the samples change with size and therefore the ice nucleating ability? Is there any bias in the measured frozen fractions due to multiple charged and therefore larger particles? A recent paper by Hartmann et al. (2016)

shows that due to commonly used particle generation methods multiple charged particles (they also used a FLUKA kaolinite sample in their study) can be present which bias the determined frozen fraction.

No, we do not know for sure the reason for the change of the contact angle distribution. In general we think that it is not unlikely that the ice nucleation ability of a given substance changes with size- that can also be seen in the active sites scheme, where an increase in size of the IN increases the chance that this IN contains an active site to trigger freezing at a specific temperature. From Fig. 9 one can thus conclude that an increase in size of the IN leads to a wider spread of possible contact angles (wider alpha-pdf distribution) and to a shift to smaller contact angles with size (because the chance to have a small contact angle increases).

For solid IN, the larger the surface area the higher the freezing temperature. This is generally the case but the change in freezing temperature with size depends logarithmic on the surface area and therefore approaches a constant temperature.

The used kaolinite sample was relatively pure, the contamination was less than 10%. Such a low contamination does not show any effect on the measurement and is negligible. We can not answer the question if the contamination level significantly changed with size.

The size selection was done with caution to prevent multiple charges. An elaborate size selection setup was used: a cascade of impactors and cyclones to reduce the amount of large particles after aerosol generation and neutralize the particles by impactions of ions followed by size selection wiht a Differential Mass Analyzer (DMA). However, multiple charges exist in the smaller size range (mainly 100 and 200 nm). The larger the particle the less they are effected by multiple charges. At a later state a CPMA was additionally included in the setup to make sure that no multiple charges exist. The mentioned updated setup was used for the microcline measurements presented in this paper.
The multiple charges were estimated for the kalonite sample (Lüönd et al. 2012?). Correcting the size accordingly and refitting the dataset shows that the uncertainty due to multiple charges is not significant. The new curves lie within the error-range of the data points. Only for the 100 and 200 nm dataset there is some deviation from the original curve.

Conclusions: I am wondering why the alpha-pdf scheme is worse compared to the other two schemes when trying to represent the measured frozen fractions as a function of temperature for the various dusts and dust sizes. But in contrast, the time dependence of freezing can only be reasonably represented by the alpha-pdf scheme. In the latter case this was shown for a given dust (kaolinite) and one size only. The questions arises again: Is there an influence of size dependent composition or multiple charged particles (see comment above) which bias the fitting as a function of T and size?

Since we only have size and time dependent measurements in case of kaolinite, it is difficult to say that the alpha-pdf scheme is in general worse than the two others. However, the reason that the formulas give better fit results in the other two cases could be only mathematical. The effect of multiple charges is negligible for the results (see answer above).

In general, the conclusion is too vague. From my point of view, this study is a good contribution in order to find appropriate parameterizations based on CNT for GCMs. But I would suggest to clearly state the limits of parameterizing the immersion freezing behavior of mineral dusts due to e.g., limited amount of data available, bias due to possible multiple charges/size-dependent particle composition issues, etc. and that further experimental studies as a function of temperature and time are needed (only one sentence, the last one on page 15, is not sufficient).

Thanks for pointing this out. We emphasized the limits/lack of experimental studies more in the conclusion.

Appendix: In general, there is no warm or cold temperature. The temperature can only be high or low. In some cases, plots/tables are shown based on f, others are based on contact angle α. It is difficult to directly inter-compare the results. Could you please refer to only one parameter or both f and α?

Indeed, thanks, this is corrected. The reason for showing sometimes f, sometimes α on the plots/tables is that the fit parameter itself is different in the different cases. It is possible to convert f to α using Eq. 3. We added the converted/approximated values of f to make a comparison easier.

1.3 Technical notes:

Page 9, line 4: the schemes are mixed up here: CNT #7 is the α(T) scheme and CNT #5 and #6 are the α-pdf schemes.

This is corrected.

Page 12, line 18: Should it read "..., which was found to not represent..."?

Yes, thanks.

Page 15, line 6: "have been compiled" instead of "are compiled"?

Done.

In the upper left plots of Fig. 7 and 8 the highest temperature value (i.e., 260 K) is truncated.

Thanks for pointing that out, that is fine now.

Figure 8, lower right panel: The mean freezing temperature is about 237 K. Does this "agree" with the high mean contact angle of 0.3?

There was a mistake in the plotting script for Fig. 7 and 8, thanks for noticing. We corrected it. Additionally we changed the values for the fixed variables (like μ) to values, which are closer to the resulting fit parameters from Table 3. The mean freezing temperature for the α-pdf scheme when using a mean contact angle of 0.5 (Fig. 8 lower panel) is approximately 239 K. That goes along with Fig. 5 (fits and measurement points for kaolinite).

Caption of Fig. 8: There is a "decreasing" missing in the sentence starting with: "contact angle gets larger with *decreasing* T because...".

Yes, thanks.

On page 33, line 5-6. There is the verb missing in the sentence "... FF is fitted or the active site density directly."

This is corrected, thanks.

Fig. 11: The color coding is less than ideal. It is difficult to see which of the lines correspond to which study.

The colors are changed now.

1.4 References:

Hartmann, S., Wex, H., Clauss, T., Augustin-Bauditz, S., Niedermeier, D., Rösch, M., and Stratmann, F. (2016), Immersion Freezing of Kaolinite: Scaling with Particle Surface Area, J. Atmos. Sci., 73(1), 263-278.

Hoose, C. and Möhler, O. (2012), Heterogeneous ice nucleation on atmospheric aerosols: a review of results from laboratory experiments, Atmos. Chem. Phys., 12, 9817-9854.

Lüönd, F., Stetzer, O., Welti, A., and Lohmann, U. (2010), Experimental study on the ice nucleation ability of size selected kaolinite particles in the immersion mode, J. Geophys. Res. – Atmos., 115(D14).

Pruppacher, H. R. and Klett, J. D. (1997), Microphysics of Clouds and Precipitation, 2. Edn., Kluwer Academic Publishers, Dordrecht.

Welti, A., Lüönd, F., Kanji, Z. A., Stetzer, O., and Lohmann, U. (2012), Time dependence of immersion freezing: an experimental study on size selected kaolinite particles, Atmos. Chem. Phys., 12(20), 9893-9907.

2 Review 2

The authors do a thorough examination of different possible ways of fitting the classical nucleation theory to immersion freezing experiments using various formulations for parameters of the theory. They compare the outcomes using three criteria: 1) How well each CNT formulation reproduces the experimental freezing curves; 2) How good are the size and time dependences of each formulation compared with experimental data (if available)? and 3) Are the values of the fit parameters microphysically reasonable? I believe that this is a useful paper that should eventually be published: at the moment CNT is the only theoretically based approach that can be used as a basis for parametrizing immersion freezing for global models, and this paper provides valuable information for constructing such parametrizations. At the same time it should be kept in mind that CNT is by no means perfect.

I have really just one major comment. The authors make the following statement in the Conclusions: ”Criterion 3 is difficult to evaluate coming from a macroscopic level as microphysical knowledge is missing at this point”. I don’t think the situation is quite that bad. There is information available in the literature that can help at least discuss whether the contact angle distributions are physically reasonable, or consistent with information gained from other studies.

First, there are molecular dynamics papers that have investigated water (both liquid and ice) especially at kaolinite surfaces (e.g. Hu and Michaelidis, Surface Science 601, 5378, 2007; ibid, 602, 960, 2008; Croteau et al., J.Phys. Chem A, 114, 8396, 2010; Solc et al., Geoderma 169, 47, 2011). Please check these and discuss how realistic the contact angle distributions derived in your study are.

We read the mentioned studies with great interest. However, only in Solč et al. 2011 a microscopic contact angle was calculated, which we could compare to our results. The derived contact angle is about 105° (that is equivalent to a geometric term f of 0.69). However, there are many assumptions needed to calculate the microscopic contact angle. Probably more simulations and a more detailed comparison is needed in future. We added some more information about molecular dynamics paper and recent investigations in the text.

Secondly, there are observations of freezing microdroplets at different hydrophopbic surfaces indicating that the contact angle does not change when freezing occurs (Jung et al., Langmuir 27, 3059, 2011; Heydari et al., J. Phys. Chem. C, 117, 21752, 2013). This information can be used in the context of Young equations. If you write down Young equations for contact angles of 1) a water cluster on a surface S, 2) an ice cluster on S (against air) and 3) an ice cluster on S, immersed in water, you can figure out what the contact angle of ice immersed in water should be if the contact angle of liquid water on the same surface is known (literature values of water contact angles can be found many minerals).

We are not sure if we understood the suggestion correctly. We used the Young equation for immersion freezing ($\cos(\alpha) = \frac{\sigma_{\mathrm{sw}}-\sigma_{\mathrm{si}}}{\sigma_{\mathrm{iw}}}$; index s stands for surface (aerosol), i for ice and w for water) to calculate the interfacial tension between a surface (aerosol) and ice for kaolinite (Young, 1805). We got values of approx. 58 mJ/m^2 at 243 K increasing by approx. 0.2 mJ/m^2/K with decreasing temperature. Similar results were already discussed by Welti et al. (2012). Because of that and since the different contact angles coming from different contact angle schemes yield approximately the same results, we do not see much value in adding this information or discussion to the paper.

Thirdly, one can make the following question (this time disregarding the assumption of equal contact angles for water and ice): Are the results in this work (i.e. contact angles of ice immersed in water) consistent (again, in the context of Young equations) with ice contact angles derived from deposition nucleation studies? This question should be answerable with the help of the different interfacial tensions used (water, ice, ice in water) and water contact angles. I suggest that you do these two exercises with the Young equations and discuss.

We calculated the contact angle for deposition nucleation from the different contact angles for immersion freezing using the following formula:

$$cos(\alpha_{\mathrm{dep}}) = \frac{cos(\alpha_{\mathrm{imm}})\sigma_{\mathrm{iw}} + \sigma_{\mathrm{sv}} - \sigma_{\mathrm{sw}}}{\sigma_{\mathrm{vi}}}\,.$$

For kaolinite the calculated contact angle for deposition freezing at 243 K is approx. 20°.

2.1 Minor:

- Contact angle values in Tables 3 and 5 don't seem consistent with the contact angle distributions in Fig. 9. Should the radian values be multiplied by π? However, even in that case, the μ-values in Fig. 10 appear a bit strange: they are mostly below 90 degrees, although the modes of the distributions in Fig. 9 are all above 90 degrees, and the distributions appear to be skewed right. How come?

  Thank you for spotting this. We phrased it wrongly what μ is and the illustration in Fig. 1 was also not correct. We wrote μ is the mean contact angle, but since it is a log-normal distribution μ is the ln of the mean contact angle instead. If you exponentiate μ and then multiply it with 180° and divide it by π you end up with the values ploted in Fig. 10. We changed the explanation for μ and adapted the illustration in Fig. 1.

  The curves in Fig. 10 are fully symmetric and not skewed- maybe you got this impression because the x-axis is chosen such that the purple distribution (920 nm) is cut?

- What happened to Appendix A?

  We are not sure if we understand that question. Appendix A can be found on page 26 and 27 (27 and 28 in the revised version; Fig. 7 and 8). We changed the references in the text directly refering to the figures.

- The order of Figs. 9 and 10 should be changed

  Done, thanks.

- The English of the ms should be checked.

  We thouroughly checked the language again and hope that the manuscript reads better now.

3 Interactive comment 1 by Peter A. Alpert

3.1 General Comments

The manuscript by Ickes et al. details the ability of different immersion freezing parameterizations based on classical nucleation theory to reproduce laboratory data. The authors target the treatment of the contact angle, α, the interfacial tension between an ice germ and water, σ_{iw}, and the activation energy barrier, $\Delta g^{\#}$. Performance of freezing parameterizations are evaluated in terms of their accuracy in reproducing measured frozen droplet fractions (criteria 1), their consistency with trends in freezing as a function of temperature, T , particle size, and time, t, (criteria 2) and finally if their fit parameters and fitting functions lead to reasonable representations (criteria 3). Comparison of formulations 1), 5) and 7) use the same thermodynamic parameterizations for σ_{iw} (Reinhardt and Doye, 2013) and $\Delta g^{\#}$ (Zobrist et al., 2007), but α is represented by different schemes namely the single-α in 1), the α-PDF in 5) and the α(T) in 7).

The manuscript in question is well written and comprehensive. The overall conclusions are justified. However, a discussion of previous literature that pertains to the performance of freezing parameterizations is lacking and alternative explanations of freezing parameterization should be explored for completeness. The authors cite Marcolli et al. (2007) and Lüönd et al. (2010) on p. 4, l. 17, however, significant advancement in comparing contact angle schemes should also be discussed and attributed to Zobrist et al. (2007), Alpert et al. (2011), Knopf and Forrester (2011), Rigg et al. (2013) and Wheeler et al. (2014). I feel that a concise discussion of the major findings in these previous studies and how the current study in question advances these findings should be presented.

Thanks for that comment. We added a section on previous literature to point out how this study conplements the earlier findings. The aim of the current manuscript is to evaluate how suitable four different CNT based schemes are for implementation in a GCM. A broad review on ice nucleation parameterizations is not within the scope of the current work.

- In Zobrist et al. (2007), a single-α scheme was evaluated for performance, but it could not reproduce the freezing of droplets due to 1-nonadecanol, an organic monolayer coating. Allowing α to be a function of T, i.e. the α(T) scheme, resulted in a good representation of their data (Zobrist et al., 2007). However, here the authors do not mention that the single-α or α(T) scheme was considered in Zobrist et al. (2007). In our recent publication (Alpert and Knopf, 2016), we address the question of the applicability of the single-α scheme to an uneven mineral dust surface, if it does not apply to uniform surface on a molecular level such as a self-assembled organic monolayer coating. In other words, a single-α was never shown to reproduce freezing data for a highly ordered and uniform surface. It has also been argued that α represents the balance of surface tensions which can change as T changes. Thus a single-α scheme is not expected to be physically applicable (Welti et al., 2012; Rigg et al., 2013).

  Differently to Zobrist et al. 2007, the schemes are evaluated to reproduce ice nucleation measurements on solid surfaces of mineral dust particles. As stated in Zobrist et al. 2007: "The experimentally determined heterogeneous ice nucleation rate coefficient (of a nondecanol monolayer) shows a much weaker temperature dependence than homogeneous ice nucleation and heterogeneous freezing in the presence of a solid ice nucleus such as Al_2O_3". Early experiments on AgI and MD simulations e.g. Cabriolu and Li (2015) support the applicability of single-alpha in certain cases. We added the references mentioned above and some further sentences about the single-α scheme in the manuscript.

- In the studies by Alpert et al. (2011), Knopf and Forrester (2011) and Rigg et al. (2013) investigating different ice nucleating particle (INP) types, it was shown that the α(T) scheme can be applied and that a linear function may be used. This corroborates findings by Zobrist et al. (2007). However, the authors neglect discussion of these studies and refer only to Welti et al. (2012).

  The change in contact angle with RH_i and temperature can be interpreted either as a result of the temperature dependence of the interfacial tensions (σ_is and σ_iw, where the index i stands for ice, w for water and s for the aerosol surface) or as the apparent contact angle of an ensemble with a diversity of contact angles from particle to particle. In contrast to the mentioned references we follow the second interpretation as was done in Welti et al. (2012). Therefore we only referenced this paper. We added some further explanation to the manuscript and added the references.

- The authors claim that parameterizations should be consistent with freezing trends of known microphysical processes (critera 3). One easily accessible microphysical process that can be discussed for evaluating freezing parameterizations is the ability to reproduce freezing point depression of aqueous solution droplets. Rigg et al. (2013) evaluated the applicability of the α-PDF and α(T) scheme to describe droplet freezing experiments. In their study, organic particles were immersed in pure water or aqueous ammonium sulfate solution droplets and freezing was observed as a function of T and water activity, a_w. The analysis demonstarted that one α-PDF distribution could not reproduce observed freezing data, but the data could be well represented allowing α to be a function of T and a_w (Rigg et al., 2013). The α-PDF scheme failed as a physical representation of the ice nucleating ability of the particles. If an α-PDF scheme is chosen to be used to describe immersion freezing in future studies, it should be modified to account for changes in a_w (Rigg et al., 2013). I suggest to include this discussion adding more detail to the authors' third criteria, how our current knowledge of microphysics can lead to more correct ice nucleation parameterizations and not only just better performance.

  Thanks, this is added in the discussion.

- Wheeler et al. (2014) evaluated many different α-schemes and found that the α-PDF is not the best performing. Instead, a scheme known as the ”active site scheme“ (AS) is the best performing. This finding should be discussed in the manuscript on p. 5, l. 28-p. 6, l. 2.

  This is added in the section refering to other studies from literature.

3.2 Specific comments:

When introducing the α schemes, there are a few instances where the author claims certainty or implies that INP surfaces have variable ice nucleation efficiency. There is no physical evidence that an INP has variable ice active sites or surfaces with different ice nucleation efficiency. For now, any evidence is a product of circumstance to a conceptual mathematical framework (or fitting procedure with prior assumptions of the existence of active sites). On p. 5, l. 2-3, the authors claim that the single-α scheme "assumes" that the surface has one α values for the entire particle surface. However, on p. 5, l. 10, the authors claim that the α-PDF "accounts" for surface heterogeneity. This later statement is incorrect. The α-PDF does not account for anything, but it does assume that the surface of particles is covered by sites that have different contact angles. In lack of in situ observations, this is not a better or more accurate assumption, but simply a different conceptual framework. The authors should state the assumptions of all schemes accurately just as they did for the single-α scheme.

You are right, all asumptions should be stated. We changed this accordingly.

On p. 5, l. 4-6, the authors claim that the α(T) scheme does not take into account how contact angles are distributed. Then say on l. 6-7 that good IN freeze first, e.g. when performing a cooling rate experiment, which shifts the mean contact angle of the remaining droplet population. These statements are contradictory as it is written. The authors say that the first scheme does not distribute contact angles, but the contact angle distribution shifts? Again, there is no certainty that a contact angle distribution exists in the first place. Rather it is sufficient to say that the α(T) scheme assumes a physical dependence of α on T. To describe this scheme as a compromise is also incorrect as it is different than the single-α and α-PDF schemes. It it is based on different assumptions and includes a physical dependence of thermodynamic parameters on α which is neglected in the other two schemes. Similarly, it also does not "reflect a changing α-PDF distribution" (l. 5-6).

We rephrased the explanation of the α(T) scheme used and hope that the additional explanation leads to less confusion. In our case the α(T) scheme is a simplified temperature dependent α-PDF scheme and not a scheme based on the physical dependence of α on T. Accounting for a physical dependence of α on T as a result of the temperature dependence of the interfacial tensions leads to a decrease of α, which is contradictory to the assumption we made here.

The authors emphasize computational efficiency, cost, expense, complexity... as a way of evaluating each scheme or parameterization. Since this is presented as a sort of metric for comparison, it should be a quantifiable metric. As it is presented by the authors here, it is not quantitative. How much time does it take for a computer to calculate σ_{iw} derived by the different parameterizations presented here? What is the extra time it takes to randomly sample from an α-PDF or calculate α(T) before freezing is predicted in a GCM? Understandably, the time it takes to fit various α schemes and other parameters is very different and may take hours is some cases. After finding all parameters and using them in formulations 1-7, how long does each take to predict ice nucleation in GCM's for the same aerosol population and thermodynamic conditions? If the authors choose to not consider the active site scheme and the soccer ball model, they must have some reason and quantitative evidence as to why. For example, p. 5 l. 31-p. 6 l. 32 claims that a scheme is too computationally expensive to be considered, but no quantitative measure is given. In order for this statement and all others like it to remain in the manuscript, the authors must provide quantitative evidence for this. Is it possible to add another column in Table 2 for this purpose?

We agree that a quantification of computational efficiency would be a nice additional information to know. However, that is not easy to derive and was therefore not mentioned explicitily. The computational time for certain freezing schemes depend on many aspects, amongst others the GCM used (treatment of aerosol particles, microphysics etc.) and can therefore not be generalised. A quantitative number in Table 2 would be meaningless.

There are some general thoughts, which can be made to assess the computational complexity of schemes before implementing them, which is the number and kind of variables needded for the scheme. In that sense an α(T) scheme is not different from a single-α scheme (same number of variables, the same number of equation have to be solved). The α-PDF scheme on the other hand is therefore more difficult as it requires an extratracer (variable, which is stored in the model longer than for one timestep) if it is implemented physically correctly. That is because the model has to memorize which contact angles from the distribution were already used in the timestep before. Otherwise the same "good" IN would be used over and over again. Using extratracer for the contact angle of mineral dust particles would approximately lead to an increase of computational costs of 21% in the GCM ECHAM6-HAM2. The depletion of contact angles can be ignored if one assumes that the aerosol particles are replenished within one time step, so that there are always the same contact angles available (if aerosol particles are available). If the time evolution of the contact angle distribution is not taken into account, the α-pdf scheme becomes computationally similarly expensive as the single-α scheme. However, the integral of the contact angle distribution can not be solved analytically. Therefore, to minimize computational costs, a look-up table could be used instead of discretized finite sums. Using look-up tables is depending on the size and format of the look-up table more expensive compared to solving an equation with simple constants as in the case of the single-α scheme. In the case of the soccer ball model it might be extensive work to create look-up tables. The computational costs are higher for the active sites scheme. It requires a memory of used contact angles in dependence of time and therefore at least one tracer variable. In many GCMs with explicit microphysics and aerosol dynamics, tracers are one of the major sources for computational time, which makes the code costly compared to other GCMs.

We added this discussion in the revised manuscript.

3.3 References

Alpert, P. A. and Knopf, D. A.: Analysis of isothermal and cooling-rate-dependent immersion freezing by an unifying stochastic ice nucleation model, Atmos. Chem. Phys., 16, 2083–2107, doi:10.5194/acp-16-2083-2016, 2016.

Alpert, P. A., Knopf, D. A., and Aller, J. Y.: Ice nucleation from aqueous NaCl particles with and without marine diatoms, Atmos. Chem. Phys., 11, 5539–5555, doi:10.5194/acp-11-5539-2011, 2011.

Knopf, D. A. and Forrester, S.: Freezing of water and aqueous NaCl droplets coated by organic monolayers as a function of surfactant properties and water activity, J. Phys. Chem. A, 115, 5579–5591,doi:10.1021/jp2014644, 2011.

Lüönd, F., Stetzer, O., Welti, A., and Lohmann, U.: Experimental study on the ice nucleation ability of size-selected kaolinite particles in the immersion mode, J. Geophys. Res., 115, D14 201, doi:10.1029/2009JD012959, 2010.

Marcolli, C., Gedamke, S., Peter, T., and Zobrist, B.: Efficiency of immersion mode ice nucleation on surrogates of mineral dust, Atmos. Chem. Phys., 7, 5081–5091, doi:10.5194/acp-7-5081-2007, 2007.

Reinhardt, A. and Doye, J. P. K.: Note: Homogeneous TIP4P/2005 ice nucleation at low supercooling, J. Chem. Phys., 139, doi:10.1063/1.4819898, 2013.

Rigg, Y. J., Alpert, P. A., and Knopf, D. A.: Immersion freezing of water and aqueous ammonium sulphate droplets initiated by Humic Like Substances as a function of water activity, Atmos. Chem. Phys., 13, 4917–4961, doi:10.5194/acpd-13-4917-2013, 2013.

Welti, A., Lüönd, F., Kanji, Z. A., Stetzer, O., and Lohmann, U.: Time dependence of immersion freezing: an experimental study on size selected kaolinite particles, Atmos. Chem. and Phys., 12, 9893?9907, doi:10.5194/acp-12-9893-2012, www.atmos-chem-phys.net/12/9893/2012/, 2012.

Wheeler, M. J., Mason, R. H., Steunenberg, K., Wagstaff, M., Chou, C., and Bertram, A. K.: Immersion freezing of supermicron mineral dust particles: Freezing results, testing different schemes for describing ice nucleation, and ice nucleation active site densities, J. Phys. Chem. A, 119, 4358–4372, doi:10.1021/jp507875q, 2014.

Zobrist, B., Koop, T., Luo, B. P., Marcolli, C., and Peter, T.: Heterogeneous ice nucleation rate coefficient of water droplets coated by a nonadecanol monolayer, J. Phys. Chem. A, 111, 2149–2155, doi:10.1021/jp066080w, 2007.

References

Cabriolu, R. and Li, T.: Ice nucleation on carbon surface supports the classical theory for heterogeneous nucleation, Phys. Rev. E, 91, 2015.

Edwards, G. R. and Evans, L. F.: Effect of surface charge on ice nucleation by silver iodide, Trans. Faraday Soc., 58, 1649–1655, 1962.

Welti, A., Lüönd, F., Kanji, Z. A., Stetzer, O., and Lohmann, U.: Time dependence of immersion freezing, Atmos. Chem. Phys., 12, 9893–9907, 2012.

Young, T.: An essay on the cohesion of fluids, Philos. Trans. R. Soc., 95, 65–87, 1805.

Classical nucleation theory of immersion freezing: Sensitivity of contact angle schemes to thermodynamic and kinetic parameters

Luisa Ickes[1*], André Welti[1+], and Ulrike Lohmann[1]

[1]Institute of Atmospheric and Climate Science, ETH Zurich, Zurich, Switzerland
[*]now at: IMK-AAF, Karlsruhe Institute of Technology, Karlsruhe, Germany
[+]now at: Leibniz Institute for Tropospheric Research, Leipzig, Germany

Correspondence to: Luisa Ickes
(luisa.ickes@env.ethz.ch)

Abstract. Heterogeneous ice formation by immersion freezing in mixed-phase clouds can be parameterized in general circulation models (GCMs) by Classical Nucleation Theory (CNT). CNT parameterization schemes describe immersion freezing as a stochastic process including the properties of insoluble aerosol particles ~~, so called ice nuclei,~~ in the droplets. There are different ways how to ~~describe~~ parameterize the properties of aerosol particles (i.e. contact angle schemes), which are compiled and tested in this paper. The goal of this study is to find a parameterization scheme for GCMs to describe immersion freezing with the ability to shift and adjust the slope of the freezing curve compared to homogeneous freezing to match experimental data.

~~The results of using~~ We showed in a previous publication that the resulting freezing curves from CNT are very sensitive to unconstrained kinetic and thermodynamic parameters in the case of homogeneous freezing~~leading to uncertainties in calculated nucleation rates J_{hom} of several orders of magnitude~~. Here we investigate how sensitive the outcome of a parameter estimation for contact angle schemes from experimental data is to unconstrained kinetic and thermodynamic parameters. We ~~show that additional free parameter~~ demonstrate that the parameters describing the contact angle schemes can mask the uncertainty ~~of J_{imm} due to~~ in thermodynamic and kinetic parameters.

Different CNT formulations are fitted to an extensive immersion freezing dataset consisting of size selected measurements as a function of ~~particle diameter (d), temperature T and time t~~ temperature and time for different mineral dust types, namely kaolinite, illite, montmorillonite, microcline (K-feldspar) and Arizona test dust. It is investigated how accurate different CNT formulations (with ~~the~~ estimated fit parameters for different contact angle schemes) reproduce the measured freezing ~~curves~~data, especially the time and particle size dependence of the freezing process. The results are compared to a simplified deterministic freezing scheme. ~~It is evaluated in this context~~ In this context it is evaluated which CNT based parameterization scheme able to represent particle properties is ~~a good~~ the best choice to describe immersion freezing in a GCM.

1 Introduction

In mixed-phase clouds freezing of cloud droplets occurs by different pathways of heterogeneous freezing/nucleation. The nucleation process is initiated on the surface of an aerosol particle, called ice nucleus (IN), which either collides with a supercooled droplet (contact freezing), acts as cloud condensation nucleus (CCN) and causes freezing when the droplet is increasingly supercooled (immersion freezing), freezes immediately after CCN activation at supercooled conditions (condensation freezing), or provides a site where water vapor deposits as ice (deposition nucleation) ~~(Vali, 1985) .~~ [Vali (1985)].

In mid latitudes, where supercooled clouds are common, IN and their effect on precipitation formation through immersion freezing influence the hydrological cycle (Lohmann, 2002; Zeng et al., 2009; DeMott et al., 2010) and thereby e.g. the biosphere and agriculture. Aerosol particles determine the formation and ice-water ratio of mixed-phase clouds, thereby the cloud radiative properties and indirectly the radiation budget, which affects earth's climate. Therefore results of climate simulations in regional and global models are sensitive to the parameterization scheme used for heterogeneous ice formation and in particular immersion freezing as it is the most abundant freezing pathway (Ansmann et al., 2009; Wiacek et al., 2010). One approach to parameterize immersion freezing in global and regional climate models is by Classical Nucleation theory (CNT)~~.~~ ~~CNT is a theory based on approximations considering~~ , which requires approximations of the thermodynamics and kinetics of nucleation. Although computationally more expensive ~~in most cases~~ compared to empirical parameterization schemes, it allows a physical treatment of ice nucleation as function of temperature T, ice supersaturation S_i , time t and IN type (e.g. size, surface properties). Using a theoretical scheme has the advantage that the scheme is valid over the whole T-S_i -space, which is mandatory for the use in a GCM, where all ~~kind~~ kinds of conditions occur (especially in certain regions like the Arctic, but also in simulations of future climate, where atmospheric conditions can be different from the present day or the pre-industrial ~~ones~~epoch). Empirical schemes are ~~in contrast~~ often limited to ~~narrow conditions~~ the narrow conditions from which the scheme was ~~estimated for~~ derived and can lead to unphysical results when extrapolated. Therefore empirical schemes might not ~~hold for future atmospheric~~ be representative for the future atmosphere or untypical atmospheric conditions. One example is the empirical Meyers et al. (1992) scheme, which was developed using measurements in ~~mid-latitude and has problems when being~~ mid latitudes and has been found to be inaccurate when extrapolated to Arctic conditions (Prenni et al., 2007).

~~The~~ Some parameters in the framework of CNT ~~is partly unconstrainedand therefore~~ are so far unconstrained. At the same time results from the CNT are very sensitive to the choice of thermodynamic and kinetic parameters, ~~namely~~ in particular interfacial tension between ice and water σ_iw and activation energy $\Delta g^{\#}$. Sensitivity of CNT on σ_iw and $\Delta g^{\#}$ in the case of homogeneous freezing has been discussed in Ickes et al. (2015). Using CNT as an approach to parameterize immersion freezing in aerosol-climate models raises the question of the sensitivity of the parameterization scheme to σ_iw and $\Delta g^{\#}$ in the case of heterogeneous freezing. Additionally there is a need to include and represent IN properties. ~~Here we use~~ We test three different schemes to describe the effect of an IN population on immersion freezing conditions and investigate the impact of the chosen scheme on the parameterization of immersion freezing. We also discuss strategies how to ~~judge/evaluate~~ evaluate the applicability of different CNT formulations.

The formalism of CNT for immersion freezing is ~~explained~~ summarized in section 2. Advantages and disadvantages of certain ~~formulation~~ formulations for the use in GCMs are discussed. In section 3 the sensitivity of the immersion freezing nucleation rate J_imm [s^{-1}m^{-2}] and the fit of the geometric term f to thermodynamic and kinetic parameters is investigated by fitting and comparing the results to an ice nucleation measurement dataset of kaolinite (Welti et al., 2012). The section is followed by suggestions for criteria how to evaluate the quality of a CNT parameterization scheme (section 4). ~~Finally in~~

~~section 5 CNT parameters are~~ Section 5 presents CNT parameters estimated from experimental data for five different mineral dust types and ~~afterwards~~ in section 5.1 the criteria ~~are tested~~ from section 4 are applied for three CNT ~~parameterization schemes~~ formulations and compared to the performance of an empirical parameterization. Throughout this paper we refer to "CNT formulations" indicating a specific CNT framework for immersion freezing based on Eq. 4, including parameterization schemes for σ_{iw}, $\Delta g^{\#}$ and the geometric term f (contact angle scheme). CNT formulation #1 as an example is later on abbreviated by CNT #1. We refer to "schemes" to discuss the different parameterization schemes for the geometric term f or the contact angle α to express the ice nucleating surface properties of aerosol particles.

2 Classical Nucleation Theory for immersion freezing

In CNT freezing is described as a stochastic process by a temperature dependent nucleation rate. In the case of homogeneous freezing (pure water droplets) statistical fluctuation of water molecules can lead to the formation of small ice-like structures (ice embryos) that lead to freezing of the supercooled droplet if they reach a certain critical size (ice germ). The nucleation rate describes the formation of ice germs leading to freezing over time. It consists of a thermodynamic and a kinetic component. The thermodynamic component describes the formation of ice embryos (determined by the thermodynamic energy barrier ΔG), the kinetic component describes the number of molecules, which can be incorporated into the ice embryo (determined by the activation energy barrier $\Delta g^{\#}$).

The presence of IN immersed in supercooled droplets facilitates ice nucleation compared to homogeneous nucleation by providing a catalytic surface. The IN ~~surfaces~~ surface reduces the thermodynamic energy barrier ΔG determined by T, S_{i} and σ_{iw}. The difference in nucleation with and without an IN i.e. homogeneous or heterogeneous nucleation, is accounted for by the geometric term f, also called wettening factor, ~~compability~~ compatibility factor or contact parameter. This term indicates the increased probability to nucleate a stable ice germ due to the presence of the IN surface ~~and therefore~~ because of the reduced number of water molecules necessary to form an ice germ. ~~It~~ f describes by how much the IN properties (of unknown nature) reduce the energy barrier for the formation of ice embryos on its surface compared to homogeneous freezing~~and can be expressed as a function of the contact angle α, which is the tangential angle between the ice embryo on the IN surface and the parent phase (here supercooled water) Fletcher (1958) :~~ :

$$\begin{aligned}\Delta G &= f(\alpha)\cdot\Delta G_{\mathrm{hom}} \\ &= f(\alpha)\cdot\frac{16\pi}{3}\cdot\frac{v_{\mathrm{ice}}^2\sigma_{\mathrm{iw}}^3}{(k_{\mathrm{B}}T\ln S_{\mathrm{i}})^2}\text{with} ,\end{aligned} \tag{1}$$

$$f(\alpha) \equiv \frac{1}{2}\left[1+\left(\frac{1-X\cdot\cos\alpha}{g}\right)^3+X^3\left(2-3\left(\frac{X-\cos\alpha}{g}\right)\right.\right.$$

$$\left.\left.+\left(\frac{X-\cos\alpha}{g}\right)^3\right)+3\cdot\cos\alpha\cdot X^2\left(\frac{X-\cos\alpha}{g}-1\right)\right]$$

with

$$X \equiv \frac{r_{\mathrm{IN}}}{r_{\mathrm{germ}}} \text{ and } g=\sqrt{1+X^2-2\cdot X\cdot\cos\alpha}\,,$$

where v_{ice} is the volume of a water molecule in the ice embryo, k_{B} ~~is~~ the Boltzmann constant, S_{i} ~~is~~ the saturation ratio with respect to ice, r_{IN} ~~is~~ the radius of the catalytic IN surface and r_{germ} ~~is~~ the critical radius of an stable ice cluster which initiates freezing of the droplet.

f can be expressed as a function of the contact angle α, which is the tangential angle between the ice embryo on the IN surface and the parent phase (here supercooled water) [Fletcher (1958)]:

$$f(\alpha) = \frac{1}{2}\left[1+\left(\frac{1-X\cdot\cos\alpha}{g}\right)^3+X^3\left(2-3\left(\frac{X-\cos\alpha}{g}\right)+\left(\frac{X-\cos\alpha}{g}\right)^3\right)+3\cdot\cos\alpha\cdot X^2\left(\frac{X-\cos\alpha}{g}-1\right)\right] \quad (2)$$

with

$$X = \frac{r_{\mathrm{IN}}}{r_{\mathrm{germ}}} \text{ and } g=\sqrt{1+X^2-2\cdot X\cdot\cos\alpha}\,.$$

The contact angle α has a value between 0° and 180°, where the latter is equal to the case of homogeneous freezing (f=1 $\rightarrow \Delta G=\Delta G_{\mathrm{hom}}$).

If the radius of the IN is significantly larger than the radius of the ice germ, ~~radius~~ curvature of the IN surface can be neglected leading to a simplified form of f (Volmer, 1939):

$$f(\alpha) = \frac{(2+\cos\alpha)(1-\cos\alpha)^2}{4}\,. \quad (3)$$

Whereas the thermodynamic term in the nucleation rate J_{imm} (thermodynamic exponent determined by the energy barrier ΔG, see above) changes from homogeneous to heterogeneous freezing, the kinetic term is assumed to be the same for homogeneous and immersion freezing. The ~~kinetics give the number of molecules, which can potentially be incorporated into the ice germ. They are captured in the~~ prefactor of the nucleation rate ~~(see Eq. 4) and the kinetic exponent (determined by the activation energy barrier $\Delta g^{\#}$). The prefactor of the nucleation rate is different in the case of immersion freezing compared to homogeneous freezing:~~ changes as well. It is defined as:

$$C_{\mathrm{prefac,hom}\,\mathrm{prefac}} = n_{\mathrm{s}}\cdot 4\pi r_{\mathrm{germ}}^2\cdot Z\cdot k_BT/h\cdot N_{\mathrm{l}}, \text{with } Z=\frac{1}{n_{k,\mathrm{germ}}}\cdot\sqrt{\frac{\Delta G}{3\pi k_{\mathrm{B}}T}}\,.$$

where n_{s} is the number of water molecules in contact with the unit area of the ice cluster, Z ~~is~~ the non-equilibrium Zeldovich factor, h the Planck's constant and N_{l} ~~is~~ the volume-based number density of water molecules in the liquid parent phase. ~~The~~

~~difference is due to homogeneous freezing being a volume-dependent process while immersion freezing is assumed to be a surface dependent process. When calculating the non-equilibrium Zeldovich factor Z, the freezing type has to be considered:~~

$$\underline{Z = \frac{1}{n_{k,\mathrm{germ}}} \cdot \sqrt{\frac{\Delta G}{3\pi k_\mathrm{B} T}}\,.}$$

Z is not the same for homogeneous and heterogeneous freezing, because the number of the water molecules in the ice germ, $n_{k,\mathrm{germ}}$, differs. As shown in Pruppacher and Klett (2000) most of the prefactors cancel out in the case of heterogeneous freezing leading to the following expression for the nucleation rate for immersion freezing:

$$J_\mathrm{imm}[\mathrm{m}^{-2}\cdot\mathrm{s}^{-1}] \;=\; n_\mathrm{s}\cdot\frac{k_B T}{h}\cdot \underline{\exp -\frac{\Delta g^{\#}}{k_\mathrm{B}T}}\,\underbrace{\exp\left(-\frac{\Delta g^{\#}}{k_\mathrm{B}T}\right)}_{\text{kinetic comp.}} \cdot \underline{\exp - \frac{f(\alpha)\cdot\Delta G}{k_\mathrm{B}T}}\,\underbrace{\exp\left(-\frac{f(\alpha)\cdot\Delta G_\mathrm{hom}}{k_\mathrm{B}T}\right)}_{\text{thermodyn. comp.}} \quad (4)$$

Since the energy barrier of immersion freezing is reduced compared to homogeneous freezing, ~~the freezing curve is shifted to higher temperatures and is less steep . This curve shift and flattening~~ J_imm is higher compared to the homogeneous nucleation rate J_hom and exhibits a different T dependence (less steep at a certain T). The shift of the freezing curve is described by the geometric term f and has to be captured by the different CNT formulations.

2.1 Parameterization schemes for the geometric term *f*

Different ~~schemes~~ parameterization schemes for f have been put forward to describe the influence of an IN on the nucleation process, i.e. to describe the ice nucleating surface properties of aerosol particles~~(Marcolli et al., 2007; Lüönd et al., 2010) .Thus when fitting experimental data the fit parameter(s) describe the physical properties of the IN~~, e.g. Marcolli et al. (2007) . Depending on the scheme ~~these~~ the IN properties are represented by functions with one or several fit parameters and the complexity for an implementation in a GCM differs accordingly. Note that increasing complexity ~~normally~~ comes with higher computational costs ~~.~~

~~Three~~ (Hurrell et al., 2009) . Based on the computational complexity we chose three schemes including one or two fit parameters ~~are used in~~ for the following sensitivity analysis (section 3)~~and~~ . They are briefly explained here followed by a paragraph about computational costs. A graphical representation of each scheme is shown in Fig. 1. For more details see Marcolli et al. (2007) and Lüönd et al. (2010).

From immersion freezing measurements the frozen fraction FF is obtained, which is the fraction of a droplet population ~~/activated aerosol population~~ that is frozen at a certain temperature T after a certain time t. To compare ~~different~~ CNT based parameterization schemes to measurements, FF is calculated from the nucleation rate J_imm. The frozen fraction FF is given by:

$$FF = 1 - \exp(-J_\mathrm{imm}(T,\alpha)\cdot A_\mathrm{IN}\cdot\Delta t), \quad (5)$$

with A_IN being the surface area of the IN. For simplicity particles are assumed to be spherical ($A_\mathrm{IN} = 4\pi r_\mathrm{IN}^2$). Thus, the surface used for the IN of a specific mass represents a lower limit (non-spherical ~~surface~~ particles would be larger).

2.1.1 Single-α scheme

The single-α scheme ~~is assigning~~ assigns one contact angle to the entire surface of ~~each particle~~all particles. It is based on the assumption that all particles have one ~~common occurrent~~ uniform surface property responsible for their ice nucleating ability. Consequently all particles have an equal probability to act as IN at given conditions. The scheme requires only one fit parameter (f or α). One variation of the single-α scheme, the single-α + fit $\Delta g^{\#}$ scheme (see section 3), requires two fit parameters (f or α and $\Delta g^{\#}$).

It is the least complex and consequently the cheapest scheme suitable ~~to implement~~ for implementation in GCMs. However, it does not take into account that ice nucleating properties might be variable throughout a particle population. This scheme is used in several models, e.g. Khvorostyanov and Curry (2000, 2004, 2005); Liu et al. (2007); Eidhammer et al. (2009); Hoose et al. (2010); Storelvmo et al. (2011); Ervens and Feingold (2012).

2.1.2 α-pdf scheme

The α-pdf scheme is an extension of the single-α scheme. It ~~accounts for the~~ assumes a heterogeneity of particles in an aerosol population by using a log-normal probability density function (pdf) for the contact angle α $p(\alpha)$. The log-normal distribution of α within a particle population is expressed by two fit parameters, the logarithmic mean contact angle μ and the variance σ of the distribution:

$$p(\alpha) = \frac{1}{\alpha\sqrt{2\pi\sigma^2}} \cdot \exp\left(-\frac{(\ln(\alpha)-\mu)^2}{2\sigma^2}\right) . \tag{6}$$

This approach attributes an individual surface property to each particle on the entire particle surface.

The variance σ ~~defines~~ accounts for the heterogeneity of the particle property within the aerosol population: the larger the variance σ, the larger the heterogeneity among the particles. The frozen fraction FF is derived by integrating the contact angle distribution over all possible contact angles:

$$FF = 1 - \int_0^{\pi} p(\alpha) \cdot \exp(-J_{\mathrm{imm}}(T,\alpha) \cdot A_{\mathrm{IN}} \cdot \Delta t)\, \mathrm{d}\alpha\ . \tag{7}$$

The approach has been frequently used to interpret freezing data, e.g. ~~Marcolli et al. (2007); Lüönd et al. (2010); Broadley et al. (2012);~~ ~~because it better represents the nature of the IN-sample.~~ Marcolli et al. (2007); Lüönd et al. (2010); Broadley et al. (2012); Welti et al. (201

Due to the increased complexity compared to the single-α scheme, only a few attempts have been made to implement it in GCMs [e.g. Wang et al. (2014)]. Application of the scheme in GCMs faces the problem of the unknown time evolution of the contact angle distribution. Because the most efficient IN will form ice first, the remaining contact angle distribution (IN, which did not freeze yet) changes in case an aerosol population is not replenished within one timestep. Without an explicit treatment of the time evolution of the ~~α-pdf~~contact angle distribution, ice formation will be overestimated since the most efficient IN can initiate freezing over and over again. The time evolution of the contact angle distribution can be neglected by assuming that the aerosol particles are replenished within one model time step. Note that this issue is closely connected to the time resolution of the GCM, which will be discussed in a future publication.

~~The frozen fraction FF is derived by integrating the contact angle distribution over all possible contact angles:~~

$$FF = 1 - \int_0^{\pi} p(\alpha) \cdot \exp(-J_{\mathrm{imm}}(T,\alpha) \cdot A_{\mathrm{IN}} \cdot \Delta t)\,\mathrm{d}\alpha\,.$$

~~Another extension~~ Another extension of the single-α and frequently used scheme is the active sites scheme, e.g. in Marcolli et al. (2007); Lüönd et al. (2010); Niedermeier et al. (2011); Welti et al. (2012); Wheeler et al. (2014). It goes one step further and assumes several surface sites with different contact angle on a single IN. ~~Freezing is described based on active sites (initiating the nucleation process), which are randomly distributed on each IN surface within the particle population. As this scheme is~~ In this case the active sites have to be memorized over several timesteps, which means that at least one extra tracer is needed in the model. This makes this scheme computationally too expensive for the use in GCMs (see section 2.1.4). Thus, it is left out ~~of~~ in the following analysis. More information about the active sites scheme can be found in Marcolli et al. (2007); Lüönd et al. (2010); Niedermeier et al. (2011).

2.1.3 Temperature dependent single-α scheme ~~(~~[$\alpha(T)$ scheme~~)~~]

The $\alpha(T)$ scheme is a compromise between the single-α and the α-pdf scheme. It ~~does not take into account how contact angles are distributed among a particle population but it is assumed~~ assumes that α is different for different T, which reflects a change of the activated fraction of the α-pdf distribution and with that a change in ~~μ with supercooling or time. This refers to the situation where good IN freeze first~~ apparent contact angle. Efficient IN (with small contact angles) freeze at highest temperatures~~shifting the mean contact angle μ of the remaining IN population to less efficient IN~~. The lower the temperature, the higher the chance that particles with larger contact angles can be activated. This leads to a change of the apparent contact angle to larger α with further cooling ~~(assuming the aerosol population does not substantially change while cooling and the contact angles are not replenished from one to the next timestep)~~due to the shift of the activated fraction of the α-pdf distribution with supercooling. The $\alpha(T)$ scheme is thus representing the shifted mean contact angle of an initial contact angle distribution, but does not take into account how contact angles are distributed among a particle population at a certain temperature. The temperature dependence of α can be approximated to be linear as discussed in Welti et al. (2012). ~~This scheme is computationally cheaper compared to the α-pdf scheme, because no integration over a contact angle distribution is necessary. It also circumvents the issue of shifting α-pdf with time, as this is inherently captured in the scheme.~~ Being capable to describe a variability of the freezing process due to a contact angle distribution without being computationally complex makes the $\alpha(T)$ scheme attractive for GCMs. However it demands an indirect assumption on how the aerosol population changes with ~~time or supercooling, respectively.~~ supercooling. It does not circumvent the issue of shifting the contact angle distribution with time.

The frozen fraction FF is estimated analogously to the single-α scheme using a linear function for $\alpha(T)$:

$$FF = 1 - \exp(-J_{\mathrm{imm}}(T, \alpha(T)) \cdot A_{\mathrm{IN}} \cdot \Delta t) \, , \tag{8}$$

with

$$\alpha(T) = \alpha_0 + m \cdot (T - 273.15\ \mathrm{K}) \, .$$

Note that in general the temperature dependence of α can be interpreted either as a result of the temperature dependence of the interfacial tensions (σ_{is} and σ_{iw}) or as the apparent contact angle of an ensemble with a diversity of contact angles from particle to particle. In contrast to Zobrist et al. (2007); Alpert et al. (2011); Knopf and Forrester (2011); Rigg et al. (2013) we follow the second interpretation (simplified temperature dependent α-pdf scheme) as explained above. Accounting for a physical dependence of α on T as a result of the temperature dependence of the interfacial tensions leads to a decrease of α, which is contradictory to the assumption we made here.

2.1.4 Computational costs

Since computational costs are strongly linked to the complexity of parameterization schemes (Hurrell et al., 2009) , the complexity of a parameterization scheme is an important factor which has to be considered before implementation into a GCM. A general quantification of the computational costs of parameterization schemes depends an many aspects (treatment of aerosol particles and cloud microphysics) of the GCM used. The number and kind of variables needed, e.g. T, size and number of a certain aerosol type, to derive J_{imm} is an indicator for the complexity of the parameterization scheme. As soon as a variable needs to be memorized over several timesteps, e.g. change in contact angle distribution, an extra-tracer is required, which might be computationally expensive.

The cheapest CNT based parameterization schemes are the single-α scheme and the $\alpha(T)$ scheme. The α-pdf scheme is computationally more expensive because the contact angle distribution changes with time if the contact angles are not replenished from one timetep to the next. An explicit treatment of time evolution of the contact angle distribution requires extratracer to memorize which contact angles from the distribution were already used in the timesteps before and thus make the scheme computationally more expensive. Using extratracer for the contact angle of mineral dust particles would approximately lead to an increase of computational costs of 21% in the GCM ECHAM6-HAM2. If the time evolution of the contact angle distribution is not taken into account, the α-pdf scheme becomes computationally similarly expensive as the single-α and the $\alpha(T)$ scheme. However, the integral in Eq. 7 can not be solved analytically. Therefore, to minimize computational costs, a look-up table could be used instead of discretized finite sums. Using look-up tables is depending on the size and format of the look-up table more expensive compared to solving an equation with simple constants as in the case of the single-α and $\alpha(T)$ scheme. The $\alpha(T)$ scheme is a simplified version of the α-pdf and computationally cheaper, because no integration over a contact angle distribution is necessary. The active sites scheme requires extratracer as well, which would lead to high computational costs (comparable to the α-pdf with explicit change of contact angle distribution with time).

3 Sensitivity analysis

3.1 Fitting immersion freezing measurements

In this section, the sensitivity of J_{imm} and FF to different combinations of σ_{iw} and $\Delta g^{\#}$ (see Ickes et al., 2015 for a discussion of these parameters) in combination with the contact angle schemes discussed in section 2.1 is analyzed by fitting and comparing the different CNT parameterization schemes to experimental data. This helps to understand how fit parameters influence the calculated ~~FF~~ freezing curves.

The experimental data taken from Welti et al. (2012) ~~consists~~ consist of optically detected frozen fractions FF of droplets containing single immersed, monodisperse kaolinite (Fluka) particles. The ~~data consists of FF~~ FF was measured as a function of T, the particle radius r_{IN} and the residence time in the measurement setup t. Experiments were performed using ~~a CFDC (ZINC/IMCA)~~ IMCA/ZINC [see Welti et al. (2012) for ~~more~~ details]. The error bars of the data reflect the uncertainty in the distinction of water droplets and ice crystals in the detection unit. For the sensitivity analysis the dataset measured after 10 s for kaolinite particles with a diameter of 400 nm is used. Note that the size of the particles might be underestimated due to the assumption of sphericity and therefore the calculated nucleation rates J_{imm} from experimental frozen fractions ~~are always the lowest estimate.~~ represent a lower limit.

To explore the sensitivity of J_{imm} ~~and FF~~ to thermodynamic and kinetic parameters ~~of CNT~~ we use different CNT formulations ~~. The~~ with thermodynamic and kinetic parameters ~~of CNT~~ from different studies. The focus is on σ_{iw}~~and $\Delta g^{\#}$ used here emerged from Ickes et al. (2015)~~. In the following all ~~approaches and different~~ CNT formulations, which are used for the analysis, are listed. An overview is given in Table 2. Capital letters in the naming indicate the author from whose publication thermodynamic and kinetic parameters are ~~used~~obtained.

#1: Single-α R&D + Z~~scheme~~

The first approach is to use a single-α scheme in combination with the thermodynamic and kinetic parameters shown to be in good agreement with homogeneous nucleation rates [see Ickes et al. (2015)]. When using a single-α scheme it ~~is~~ might be important that the kinetic and thermodynamic parameters are a combination which reproduces the homogeneous freezing data well as there is only one fit parameter and ~~uncertainties~~ deviations cannot be compensated by additional parameters. The emerged best fitting combination of σ_{iw} and $\Delta g^{\#}$ ~~(derived independently of J)~~ from the analysis of homogeneous data is σ_{iw} from Reinhardt and Doye (2013) and $\Delta g^{\#}$ from Zobrist et al. (2007). It is tested if these formulations of σ_{iw} and $\Delta g^{\#}$ are also applicable to reproduce heterogeneous nucleation rates ~~with assumptions of~~ in combination with the single-α scheme.

#2: Single-α R&D + fit $\Delta g^{\#}$~~scheme~~

An second approach which emerged from Chen et al. (2008) is using a constant $\Delta g^{\#}$ as an additional fit parameter to f/α instead of taking a temperature dependent formulation. This assumption might be wrong in the context of homogeneous freezing especially at very low T (Barahona, 2015). However, it should be applicable for immersion freezing conditions as the change in $\Delta g^{\#}$ is small in the corresponding temperature range. The approach is used in combination with σ_{iw}

from Reinhardt and Doye (2013) and a single-α scheme. To decide if σ_{iw} from Reinhardt and Doye (2013) is the best choice, different expressions for σ_{iw} ~~(derived independently of J)~~ are tested against a fit of the homogeneous nucleation rate J_{hom} using constant $\Delta g^{\#}$ (see Fig. 2 ~~analog~~ analogous to Fig. 17 in Ickes et al.,2015). We find that σ_{iw} from Reinhardt and Doye (2013) remains an appropriate choice even when $\Delta g^{\#}$ is used as a constant.

#3 and #4: **Single-α O + fit $\Delta g^{\#}$ ~~scheme~~ and single-α E + fit $\Delta g^{\#}$~~scheme~~**

~~For the sensitivity study of J_{imm} to the kinetic and thermodynamic parameters the focus is on σ_{iw}.~~ To capture the whole possible range, two formulations of σ_{iw} are used. One from Eadie (1971) leading to the lowest homogeneous nucleation rate and a second formulation of σ_{iw} from Ouchi (1954) leading to the highest homogeneous nucleation rate (see Fig. 2). For a summary of the two formulations of σ_{iw} we refer to Ickes et al. (2015).
These two extremes of σ_{iw} are used together with a constant $\Delta g^{\#}$ (fit parameter) and the single-α scheme to clarify if a fit of α can compensate for a low/high σ_{iw}.

#5: **α-pdf R&D + Z~~scheme~~**

This ~~scheme~~ CNT formulation is an α-pdf scheme using the same thermodynamic and kinetic parameter as the CNT formulation for the single-α scheme (CNT #1). ~~This~~ The α-pdf increases the complexity and adds an additional fit parameter compared to the single-α R&D + Z ~~scheme~~ formulation (#1). ~~By doing this~~ Thus we test the influence of the choice of the contact angle scheme on the fit result. Additionally we examine if the number of free fit parameters ~~plays a role when choosing a contact angle scheme~~has an impact on the result.

#6: **α-pdf E + Z~~scheme~~**

One extreme formulation of σ_{iw} from Eadie (1971) is used together with $\Delta g^{\#}$ from Zobrist et al. (2007) and the α-pdf scheme (see #5.).

#7: **$\alpha(T)$ R&D + Z~~scheme~~**

Similar to the α-pdf R&D + Z ~~scheme (~~formulation (CNT #5), thermodynamic and kinetic parameter from the formulation for the single-α scheme (CNT #1) are used with an $\alpha(T)$ scheme instead of the single-α scheme.

The dataset from Welti et al. (2012) is fitted with the ~~previous~~ previously listed CNT formulations. The fits are done by least-square minimization of FF as a function of T. The results are shown in Fig. 3 and Table 2. Table 2 additionally contains ~~a summary of the CNT formulations~~information on $\Delta g^{\#}$ and σ_{iw}. Overall most CNT formulations with two fit parameters are able to capture the freezing ~~curve~~ data well with similar root mean square errors (RMSE) of the estimated freezing curve and measured freezing ~~curve independent~~ data independently of the thermodynamic and kinetic parameters. In the following the results are discussed in more detail.

The single-α R&D + Z ~~scheme (~~formulation (CNT #1) poorly captures the experimental data and results in a too steep freezing curve. With the single-α scheme it is not possible to reproduce the reduction of the energy barrier in a correct manner and to decrease the temperature dependence of the nucleation rate from the homogeneous to the heterogeneous case. Having only one fit parameter, which in this case is a factor in the exponential term, is not sufficient to shift and flatten the freezing curve compared to homogeneous freezing. Only the T-shift of the freezing curve compared to homogeneous freezing is captured by the fitted single-α scheme. This can be seen in a more general illustration in Fig. 7 and Fig. 8 (App. A). This result indicates that the simplified assumption of ~~a homogeneous (single)~~only reducing ΔG by a single contact angle for the entire population is not sufficient. However, early experiments on AgI and recent molecular dynamics simulations [e.g. Cabriolu and Li (2015)] support the applicability of single-α in certain cases. Possibly a single-α scheme can be used for highly efficient IN triggering ice formation at low supercooling. In the context of the Young equation (Young, 1805) the assumption of a single-α scheme is questionable. If α represents the balance of the three surface tensions it has to change with T since the surface tensions are temperature dependent.

Using $\Delta g^{\#}$ as an additional fit parameter (~~scheme~~ CNT #2) ~~reduces the steepness of~~ can flatten the curve. In this case both fit parameters are factors in the exponential term of the nucleation rate with a similar influence on the fitted FF. The fit parameter which is multiplied with the temperature dependent variable ΔG (f) mainly shifts the freezing curve but cannot reduce the steepness sufficiently at the same time (see single-α scheme). Using a second fit parameter $\Delta g^{\#}$ resolves this issue. A simplified view on this is ~~,~~ that one fit parameter is responsible for the shift ~~,~~ and the other one for the flattening of the immersion freezing curve compared to homogeneous freezing. Using a constant $\Delta g^{\#}$ might be reasonable based on the results from the homogeneous freezing analysis (Ickes et al., 2015), but fitting $\Delta g^{\#}$ to immersion freezing data leads to substantially higher $\Delta g^{\#}$ than those estimated by theoretical calculations (see Ickes et al., 2015). Moreover the fit value of $\Delta g^{\#}$ is aerosol-specific. This might be an artificial result and it is questionable if the assumption of a temperature independent and aerosol type specific (due to the fitting) $\Delta g^{\#}$ is a physical valid approach. It contradicts the assumption that the kinetic parameters such as $\Delta g^{\#}$ are the same for homogeneous and heterogeneous nucleation. The general approach to take the same thermodynamic and kinetic parameters (besides f and the prefactor) for homogeneous and heterogeneous nucleation is based on the assumption that mechanisms (e.g. the diffusion of water molecules across the water-ice boundary) in the supercooled water are not influenced by the immersed aerosol particle. This hypothesis might not be true. ~~The aerosol~~ The aerosol particle might influence e.g. the diffusion of water molecules close to the particle which could ~~explain~~ justify a change in $\Delta g^{\#}$ depending on aerosol type. A disturbance of the diffusion by an aerosol particle could e.g. be related to an impact on the hydrogen bond network by IN surface charges or polarizability of the particle surface (Edwards and Evans, 1962) .

An alternative to having $\Delta g^{\#}$ as an additional fit parameter is to use a more sophisticated contact angle scheme, e.g. the ~~$\alpha(T)$~~ α-pdf scheme (CNT #5 and #6) or the ~~α-pdf~~ $\alpha(T)$ scheme (CNT #7). Both approaches lead to good ~~agreement with~~ fits of the experimental freezing ~~curve~~ data and can be physically justified because they resemble the natural variability of ~~IN by assuming a contact-angle distribution (in the case of $\alpha(T)$ only indirectly)~~an IN population. The $\alpha(T)$ scheme has the disadvantage that it is not ~~known how~~ inherently known how the apparent α changes with T. A wrong assumption could lead to an unphysical contact angle scheme~~, where the change of α does not represent the shift in the contact angle distribution correctly~~.

The curves resulting from ~~scheme~~ CNT #3-7 (single-α + fit $\Delta g^{\#}$ schemes, α-pdf schemes and $\alpha(T)$ scheme) all support the hypothesis that increasing the number of fit parameters from one to two allows to find a reasonable fit, independent of the kinetic and thermodynamic parameters chosen and also independently of the contact angle scheme. This ~~hypothesis~~ is also supported by the result of the single-α scheme, where one fit parameter alone cannot shift and flatten the freezing curve. However, using a single-α scheme with a different additional fit parameter (e.g. the slope of σ_{iw} instead of a constant $\Delta g^{\#}$) does not lead to a better fit of the freezing curve. This might be due to the formula ~~for~~ of the energy barrier preventing a ~~sufficient~~ sufficiently large influence of the additional fit parameter on the steepness of the curve. $\Delta g^{\#}$ as an additional fit parameter is able to reduce the steepness of the freezing curve as it has the opposite temperature dependence compared to the energy barrier ΔG. For a visualization of how the fit parameters influence the freezing curve for each scheme~~see~~, please see Fig. 7 and Fig. 8 (App. A).

Using one CNT formulation, e.g. the single-α R&D + fit $\Delta g^{\#}$ ~~scheme (~~formulation (CNT #2) together with ~~wrong fit parameters~~fit parameters, e.g. α, emerging from a fit ~~from~~ with a different CNT formulation, e.g. the single-α E + fit $\Delta g^{\#}$ ~~scheme (~~formulation (CNT #4) leads to a wrong freezing curve~~. This~~, which is illustrated in Fig. 3 [solid red line, single-α R&D + fit $\Delta g^{\#}$(E) (#2/4)]. It is an example of the implication if fit parameters are used together with a different CNT formulation, that was not the one used to derive the fit parameters. This can unintentionally happen in GCMs if an implemented CNT formulation is later extended, e.g. by another aerosol species, and no care is taken that the fit parameters for the new species from the literature are derived from the same CNT formulation as the one implemented in the model.

~~Being able to reproduce experimental data does not directly depend on σ_{iw} and $\Delta g^{\#}$ and not only on the number of fit parameters used, but also on the contact angle scheme. In a reverse conclusion this means that the fit results of α, α_0 and m or μ and variance σ strongly depend on the CNT formulation used.~~ Looking at Table 2 one can see that f differs substantially, e.g. when using the single-α + fit $\Delta g^{\#}$ scheme with different ~~assumptions of~~ values for σ_{iw}. Comparing σ_{iw} from Reinhardt and Doye (2013) with σ_{iw} from Ouchi (1954) leads to a difference in fitted f of more than 300%, which translates into a difference in contact angle α of approx. 75°. However, all single-α + fit $\Delta g^{\#}$ schemes result in a nearly similar freezing curve with the same RMSE. The fit parameters from the contact angle scheme compensate inaccuracies ~~coming~~ associated with from thermodynamic and kinetic parameters and thus mask potentially wrong assumptions, e.g. ~~of the most important, unconstrained parameter in CNT of homogeneous freezing,~~ σ_{iw} of Ouchi (1954) . This makes it challenging to compare contact angles or fit parameters from different studies if not the same CNT formulation was used. Hence in the next subsection we investigate how fit results vary when thermodynamic and kinetic parameters differ and if there is a possibility to compare fit parameters from different studies using different CNT formulations.

3.2 Uncertainty of fitting α and α-pdf

Table 2 shows that, dependent on the choice of σ_{iw} and $\Delta g^{\#}$, the estimated fit parameters differ. ~~The choice of thermodynamic and kinetic parameters (σ_{iw} and $\Delta g^{\#}$) influences the fit results of different contact angle schemes, which makes comparisons of studies difficult. A~~ As an example, a contact angle estimate ~~can be different when~~ using CNT with e.g. σ_{iw} from Pruppacher and Klett (2000) compared to using ~~CNT with~~ σ_{iw} from Zobrist et al. (2007) leads to different results. In this section the sensitivity of two ~~contact-angle~~ contact angle schemes to σ_{iw} and $\Delta g^{\#}$ is investigated.

The two CNT formulations used in this analysis are a single-α R&D + fit $\Delta g^{\#}$ ~~scheme (~~formulation (CNT #2) and the α-pdf R&D + Z ~~scheme (~~formulation (CNT #5) described ~~above~~in sect. 3.1. We chose these two ~~schemes because scheme~~ formulations because CNT #2 is used in GCMs and ~~scheme~~ CNT #5 to interpret our data. Both schemes contain two fit parameters (f and $\Delta g^{\#}$ in ~~scheme~~ CNT #2, μ and variance σ of the contact angle distribution in ~~scheme~~ CNT #5). We analyze how ~~these~~ the two fit parameters depend on a change in thermodynamic and kinetic parameters. For this purpose the thermodynamic and kinetic parameters are varied up to ± 50%. For ~~the scheme~~ each variation (e.g. an increase of σ_{iw} by 10%) fitting is done to the same immersion freezing data from Welti et al. (2012) as in the previous section. For the CNT #2 the thermodynamic parameter σ_{iw} is varied, for the ~~scheme~~ CNT #5 the thermodynamic and kinetic parameters σ_{iw} and $\Delta g^{\#}$ are varied separately. The resulting fits are then compared to the reference fit results of section 3.1 (see Table 2). ~~For each variation (e.g. an increase of σ_{iw} by 10) fitting is done to the same immersion freezing data from Welti et al. (2012) as in the previous section. Figure 4a) shows the relative change of the fit parameters as a function of percentual change in σ_{iw} for scheme~~

In both cases (CNT #~~2. The higher the variation of σ_{iw} the larger is the deviation in f from the estimated fit parameters to the reference fit value, whereas $\Delta g^{\#}$ remains unchanged. Fig. 4b) shows the relative change of the fit parameters as a function of percentual change in σ_{iw} and $\Delta g^{\#}$ for scheme~~ 2 and #~~5. In both cases~~ 5) a similar change in fit parameters can be seen. Changing the thermodynamic parameter σ_{iw} has a stronger impact on the fit parameters than changes in the kinetic parameter $\Delta g^{\#}$~~see scheme 5 (Fig. 4 b)~~. This is expected from the nucleation rate formula, where σ_{iw} enters the calculation of the nucleation rate to the power of three and therefore changes the nucleation rate ~~/~~or frozen fraction more drastically than a change in $\Delta g^{\#}$.

In case σ_{iw} is increased/overestimated, the fit parameters are decreasing to compensate the change (see dashed arrow in Fig. 4a) and conversely (see dotted arrow in Fig. 4a). The behavior of this compensation is not symmetric but follows the structure of the nucleation rate formula, i.e. $1/x$ dependence for f or μ and variance σ, respectively. That implies that the change in the fit parameter gets larger the larger the variation of σ_{iw} is. The relative change approaches ~~-100~~negative 100% with increasing σ_{iw}. A larger deviation can be seen for the case where σ_{iw} is decreased/underestimated. ~~Note that in scheme~~

Figure 4a) shows the relative change of the fit parameters as a function of percental change in σ_{iw} for CNT #~~2 (Fig. 4 a) only~~ 2. The higher the variation of σ_{iw} the larger is the deviation in f from the reference fit value, whereas $\Delta g^{\#}$ remains unchanged. Only one fit parameter (f) is compensating the change in σ_{iw}~~, which is due to the stronger impact~~. Looking at Eq. 1 and 4 the product of f ~~than $\Delta g^{\#}$ on~~ and σ_{iw}^3 enters the exponential of the thermodynamic part of Eq. 4. As long as $f \cdot \sigma_{\mathrm{iw}}^3 = \text{constant}$ the resulting nucleation rate J_{imm} ~~.~~is the same. Therefore $\Delta g^{\#}$ is not sensitive to a deviation of σ_{iw}.

Figure 4b) shows the relative change of the fit parameters as a function of percental change in σ_{iw} and $\Delta g^{\#}$ for CNT #5. In case $\Delta g^{\#}$ is changed (~~only in~~ Fig. 4b) the compensation is linear for μ, following the structure of the nucleation rate formula. For σ the compensation is linear for small changes of $\Delta g^{\#}$ (until a change of approximately 30%), but is nonlinear for larger variations of $\Delta g^{\#}$.

Summarizing, an over/underestimation of σ_{iw} has a strong effect on the value of the resulting fit parameter, while ~~an~~ the effect of over/underestimation of $\Delta g^{\#}$ is ~~less severe~~small. If fit parameters were estimated based on fitting different CNT formulations they can not be directly compared. Fig. 4 can be used to estimate how different fit parameters would ~~look like~~

change due to different assumptions for σ_{iw} or $\Delta g^{\#}$. ~~Some concrete examples/numbers how different fit parameter would look like if~~ An example how fit parameters change with different CNT formulations ~~are used for the fit are shown~~ is given in Appendix B.

4 ~~How~~ Strategy to evaluate different CNT formulations~~?~~

The sensitivity analysis in section 3 ~~raises the question how to evaluate different CNT formulations. Since~~ shows that most CNT formulations with at least two fit parameters are able to reproduce ~~the freezing curve of the measurements, it is not possible to use this reproducibility or goodness of the fit as the only measure for the physical capability of the used CNT formulation. In practice, mostly, contact~~ measured freezing data. Contact angle schemes are mostly judged based on the RMSE of the estimated freezing curve and measured freezing ~~curve~~data. Only looking at the reproducibility of freezing ~~curves howevermight be not conclusive enough~~ data, however, is not a conclusive measure of how well immersion freezing is represented, since the fit parameters can mask uncertainties in the thermodynamic and kinetic parameters of CNT. ~~Therefore, the evaluation of~~ We propose to evaluate different CNT formulations ~~has to be done by stepwise~~ by testing different fit properties against measurements. The evaluation consists of a macroscopic and a microscopic perspective. ~~Together, both perspectives yield three criteria~~ Three evaluation criteria are suggested.

At ~~the~~ a macroscopic level: Is the CNT formulation capable of reproducing the measured ~~FF at a given temperature~~ T-dependence of FF and how well is ~~the~~ dependence on IN size and time ~~dependence captured? The primary factor to test is~~ captured? According to the sensitivity of immersion freezing on T, r_{IN} and t, the representation of the temperature dependence, followed by the size of the IN and the predicted time dependence of the freezing process ~~. All three dependencies~~ should be captured by a suitable CNT formulation if it is used as a function of T, r_{IN} and t in a GCM.

When evaluating fits to ~~measured freezing curves~~ a dataset that contains freezing data as a function of T, r_{IN} and t the goodness of the fit implicitly ~~contains~~ includes all three aspects~~(dependence on T, r_{IN} and t)~~. However, because T has the strongest effect on the FF , the goodness of fit mostly reflects how well the CNT ~~scheme~~ captures the temperature dependence. Two criteria emerge from the macroscopic level:

Crit. 1 How accurately can the overall freezing ~~curves~~ data be reproduced, i.e. how well is the temperature dependence of the FF captured by the CNT formulation?

Crit. 2 How accurately are the particle size and time dependence of the freezing process captured by the CNT formulation? Criterion 2 can only be investigated if time and ~~/or~~ particle size dependent measurements are available.

At ~~the~~ a microscopic level: Do the fit parameters match the microphysical assumptions of CNT ~~, i.e. are the fit parameters~~ and are they in general physically reasonable? To evaluate if ~~derived~~ fit parameters are physically reasonable, the analysis of heterogeneous freezing can be combined with ~~the~~ findings from homogeneous freezing. Including homogeneous freezing into the analysis might be useful because of ~~less~~ fewer unconstrained parameters in this case.

The microscopic criteria to be tested is:

Crit. 3 Are the values for the fit parameters reasonable in the context of what we know about the microphysical process of nucleation?

In the following these three criteria are used to decide which CNT formulations are suitable for parameterizing immersion freezing, e.g. in a GCM.

5 Using experimental data to estimate CNT parameters for different contact angle schemes

In the following a comprehensive dataset of FF (different aerosol species, aerosol particle sizes and residence times in the ~~cloud chamber~~experiment) is used. Five different mineral dust types were chosen for the analysis: Fluka kaolinite, illite-NX, montmorillonite, microcline (K-feldspar) and ATD (Arizona test dust). Montmorillonite or kaolinite are often used in global models as a surrogate for ~~ice nucleating dust~~ mineral dust in terms of ice nucleation, e.g. montmorillonite in ECHAM6-HAM2. ~~They both represent clay minerals with kaolinite being a rather inefficient clay IN and montmorillonite an efficient clay IN.~~ Fluka Kaolinite, which was used here, has been widely used to study the mechanism of immersion freezing. Illite-NX was chosen ~~by the INUIT community~~ as a the mineral dust reference sample ~~, e.g. for~~ for an instrument intercomparison (Hiranuma et al., 2015). ~~Microcline (a~~ A microcline sample from Namibia ~~, variation Amazonit) and ATD were~~ and ATD are included to enable sensitivity studies of the freezing parameterization scheme with more efficient IN. The ~~experiments were done by A. Welti (Welti et al. (2012) and personal communication)~~ experimental data for kaolinite is taken from Welti et al. (2012) . Illite-NX data has been published in Hiranuma et al. (2015) . Microcline, montmorillonite and ATD data are new datasets. All measurements were performed using size-selected aerosol particles with diameters of 50, 100, 200, 400, 800 and 920 nm and 10 s residence time. ~~Additional kaolinite measurements were done~~ The kaolinite dataset contains time dependent measurements for different residence times of 1, 2, 3, 6, 9 and 21 s. Note that the residence times are rounded to full seconds [compared to Welti et al. (2012)] and not all datasets include the smallest and/or largest size (kaolinite: 100 - 920 nm, illite 100 - 800 nm, montmorillonite 100 - 800 nm, microcline 50 - 800 nm, ATD 100 - 800 nm). The error bars of the data reflect the detection uncertainty and the statistical uncertainty in the measurement by multiple measurements.

To ~~estimate the parameters of~~ derive fit parameters for the CNT parameterization scheme four CNT formulations are chosen: #1 [single-α scheme], #2 [single-α scheme with $\Delta g^{\#}$ as a fit parameter], #5 [α-pdf scheme] and #7 [$\alpha(T)$ scheme]. For more details see Table 2. ~~Scheme~~ CNT #3, #4 and #6 use a σ_{iw}, which was found ~~not to~~ to not represent homogeneous freezing well ~~.~~ and are excluded based on criterion 3. The wrong assumption of σ_{iw} was chosen on purpose for the sensitivity study in section 3.1 to demonstrate how that influences the fit results and the freezing curves. ~~In the context of this section these formulations are excluded because they do not fulfill criterion 3.~~ Note that also the single-α R&D + Z ~~scheme (~~formulation (CNT #1) is not expected to be able to reproduce the experimental freezing ~~curves (criterion~~ data (Crit. 1). It is still included here for comparison of the RMSE value with the other formulations (“bad” reference).

The fit parameters are determined by least square minimization of the calculated versus measured FF ~~from the dataset~~. For this purpose the dataset of each dust species, including all measurements as a function of T, ~~aerosol particle size (diameter d) and residence time (~~r_{IN} and t~~)~~, is used. To get an impression of the variability of the fit parameters throughout a dataset, the kaolinite dataset is ~~additionally~~ fitted for each size and time separately in Appendix C.

The fit parameters for the different CNT formulations and aerosol types are shown in Table 3 together with the best fit root mean square error (RMSE). The fit curves in comparison to the measured FF are shown in Fig. 5 to Fig. 6 (in the case of kaolinite only a selection of the data is shown).

The geometric term f in Table 3 is smallest for microcline, showing that this is the most efficient IN investigated here. The second lowest value for f is found for ATD. Montmorillonite and kaolinite seem to be quite similar in terms of IN efficiency, whereas illite is the least efficient IN.

Revising the fit results with criterion 1 shows that ~~scheme~~ CNT #1 is too steep and not able to reproduce experimental data, resulting in a high RMSE. One fit parameter is not enough to shift and reduce the steepness of the immersion freezing curve sufficiently compared to homogeneous freezing. Thus the single-α scheme (CNT #1) does not fulfill criterion 1. Reasonable fit results (low RMSE) are obtained with ~~scheme~~ CNT #2 and #5 for all datasets. ~~It is difficult to fit the data with scheme~~

In the case of CNT #5 the mean contact angle is very similar to the contact angle of CNT #1, i.e. the medium freezing temperature (FF =0.5) is similar, but the steepness of the freezing curve is reduced by the variance of the contact angle distribution σ. See App. A for additional analysis on the influence of μ and σ on the fit of FF .

When fitting CNT #7 ~~since there is~~ more than one solution for fit parameters is found (no absolute minimum of the fitting function). However, α_0 should ~~not become negative~~ be positive and m has to be negative so that α increases with decreasing T. Otherwise criterion 3 is not fulfilled. Here only the fit parameters that ~~fullfill~~ fulfill criterion 3 are ~~given~~ reported (local minimum of the fitting function).

~~Over~~ For all CNT formulations, the fits with largest RMSE are the ones for ATD which is probably caused by ~~the mixed~~ a size dependent mineralogy of ATD. The ~~capability of the different CNT formulations to best reproduce~~ CNT formulation that best reproduces immersion freezing varies from dust to dust. Therefore, we establish a ranking for each dataset similar to the methodology ~~of~~ used in Wheeler et al. (2014). The best CNT formulation gets a ranking of 1, the worst a ranking of 4. From the ranking of the different datasets an average ~~score is estimated~~ ranking is derived to judge the overall capability to predict FF for each CNT formulation. The ranking (see Table 4) shows that ~~scheme~~ CNT #7 and ~~scheme~~ CNT #2 are the best followed by ~~scheme~~ CNT #5 and ~~scheme~~ CNT #1. Calculating the average RMSE from all fits (as an alternative) leads to ~~a similar~~ the same result, where ~~the scheme~~ CNT #7 is the best and ~~scheme~~ CNT #1 ~~)~~ the worst (see also Table 4).

Note that this ranking does not consider criterion 2 and 3 and is only based on fit statistics. It also does not show directly how good the CNT formulations reproduce time and particle size dependence of the freezing process (~~criterion~~ Crit. 2).

In section 5.1, the time and size dependence of the best three CNT formulations ~~(scheme~~ (CNT #2, ~~scheme~~ CNT #5 and ~~scheme~~ CNT #7) are compared to the kaolinite dataset. A deterministic immersion freezing parameterization scheme based on Niemand et al. (2012) is included in the evaluation for comparison (for more details on the deterministic parameterization scheme see Appendix D). ~~This~~ The Niemand et al. (2012) scheme is frequently used in literature for comparing laboratory measurements, e.g. Atkinson et al. (2013); Hoffmann et al. (2013); Kanji et al. (2013); O'Sullivan et al. (2014); Tobo et al. (2014); Umo et al. (2015), but also as a parameterization scheme in ~~some cases~~model studies, e.g. ~~Barahona et al. (2014); ?); Hande et al. (2015) .~~ Barahona et al. (2014); Paukert and Hoose (2014); Hande et al. (2015) .

6 ~~Testing the time and particle size dependence (Criteria 2)~~

5.1 Testing the time and particle size dependence (Criteria 2)

To test the ability of the single-α R&D + fit $\Delta g^{\#}$ ~~scheme (~~formulation (CNT #2), the α-pdf R&D + Z ~~scheme (~~formulation (CNT #5) and the $\alpha(T)$ R&D + Z ~~scheme (~~formulation (CNT #7) to reproduce experimentally observed size and time dependence, the fit parameters for kaolinite (see Table 3) are used to calculate FFs for three different residence times (1, 10 and 21 s) and three different aerosol particle diameters (100, 400, 800 nm). In the case of the size dependent calculation of FF the time is 10 s, in the case of the time dependent calculation the aerosol particle diameter is 400 nm. The calculated FF is compared to measurements of the size and time dependent FF in Fig. 5. The analysis of the RMSE ~~for each dataset~~ of the fit for each subset of data and CNT formulation revealed marginal differences in the second decimal place and is therefore not ~~shown.~~ reported.

Figure 5 ~~shows that scheme~~ shows that CNT #5 is able to ~~represent~~ capture the time and particle size dependence better than ~~scheme~~ schemes #2 and #7. This leads to an overall smaller RMSE and explains the better ranking for ~~scheme~~ CNT #5 in the case of kaolinite (see Table 3). Looking at Fig. 5, ~~the scheme~~ CNT #2 and #7 ~~seem to~~ give very similar results which overpredict both the size and time dependence, while ~~scheme~~ CNT #5 seems to underpredict the particle size dependence but captures the time dependence well. Overpredicting the size dependence translates into an overestimation of FF for particles with an aerosol particle diameter larger than 400 nm and an underestimation of FF for particles with an aerosol particle diameter smaller than 400 nm. Underpredicting the size dependence has the opposite influence on FF . Overpredicting the time dependence means that FF is overestimated ~~having a larger timestep (~~when using a timestep larger 10 s ~~)~~ as in GCMs.

~~Note, that the~~ The outcome of the evaluation depends on the dataset used. For different aerosol species the ranking of ~~scheme~~ CNT #5 and ~~scheme~~ #2 differs, e.g. for montmorillonite, microcline and ATD. Due to this limitation, it cannot generally be concluded which contact angle scheme ~~better~~ best fulfills criterion 2. ~~Since all three schemes are computationally equally expensive (if the contact angle distribution is not changed with time), they all might~~ All three schemes might thus be chosen for CNT based immersion freezing parameterization schemes in GCMs. The computationally least expensive formulations to use in a GCM would be CNT #2 and #7.

In Fig. 5 the CNT curves are also compared to an empirical immersion freezing parameterization scheme ($n_{\mathrm{s,IN}}$ scheme) based on the expression given in Niemand et al. (2012) ~~. Since the scheme is dependent on the measurement data used to derive it, the use for comparison is only limited. To be able to compare an empirical scheme to the CNT schemes, a $n_{\mathrm{s,IN}}$ scheme similar to the one in Niemand et al. (2012) was fitted to kaolinite measurements. Details can be found in~~ fitted to the kaolinite measurements (for details please see Appendix D). The $n_{\mathrm{s,IN}}$ scheme slightly overestimates the particle size dependence and the scheme does not ~~capture~~ include any time dependence since it is deterministic. ~~It is able to represent freezing curves in a similar manner as CNT~~ Derived FF curves appear similar to CNT curves. However, due to the general characteristics of empirical relations it is not clear if it can be extrapolated to a wide T-range, which would be mandatory for the use in a GCM.

5.2 Testing the physical reasonability of fit parameters (Criteria 3)

Since our knowledge about the microphysical behavior of supercooled water is limited, and measurements on the microscopic level are very difficult, the evaluation of the reasonability of the fit parameters is challenging. Homogeneous freezing measurements or results for molecular dynamics simulations can be used to additionally evaluate certain CNT formulations and contact angle schemes. Molecular simulations recently started to simulate heterogeneous freezing, often using kaolinite surfaces (Hu and Michaelides, 2007, 2008; Croteau et al., 2010; Šolc et al., 2011) . Hu and Michaelides (2007, 2008) found, that the ice nucleation ability of kaolinite results from the amphoteric nature of the surface hydroxyl (OH) groups, meaning that these OH groups can act as hydrogen bond acceptors or donators. The surface hydroxyl groups are reacting flexibly to the orientation of the water molecules above the surface. Therefore water molecules bonding more easily with the kaolinite surface compared to other water molecules form an ice-like stable system. Such information can be used to understand the effect a particle surface can have on the kinetics of ice formation. The study of Šolc et al. (2011) is an example for a molecular simulation study that could help to evaluate fit parameters. Šolc et al. used force-field molecular dynamics simulation to investigate water nanodroplets on a kaolinite surface and estimated a microscopic contact angle of approx. 105°. That is equivalent to a geometric term f of 0.69 (Eq. 3). Unfortunately none of the results for the different CNT formulations in our study is close to this value.

5.3 Comparison to other studies

Several previous studies investigated the capability of different CNT formulations to correctly reproduce measured freezing data for different IN, e.g. Zobrist et al. (2007); Marcolli et al. (2007); Lüönd et al. (2010); Niedermeier et al. (2011); Alpert et al. (2011); K some of them investigating contact angle schemes comparable to the ones in this study.

In all studies (including the present one) the single-α scheme does not represent the measured freezing data very well (only when $\Delta g^{\#}$ is used as an additional fit parameter). Even in the recent study of Alpert and Knopf (2016) the single-α scheme is not able to reproduce the freezing curve of a uniform surface (organic monolayer coating). The single-α + fit $\Delta g^{\#}$ scheme has not been evaluated against other schemes in the above mentioned studies. The ranking of the $\alpha(T)$ and α-pdf scheme differs from study to study. In Zobrist et al. (2007); Alpert et al. (2011); Knopf and Forrester (2011); Welti et al. (2012); Rigg et al. (2013) an $\alpha(T)$ scheme leads to good results. For all investigated IN (kaolinite, organic IN and marine biogenic IN) α is increasing with decreasing T in the mentioned literature. Note that in the study of Zobrist et al. (2007); Alpert et al. (2011); Knopf and Forrester (2011); Ri temperature dependence of α is based on the change in interfacial tensions with T (according to Young (1974)).

The α-pdf scheme did not produce good results in the study of Rigg et al. (2013) (aqueous ammonium sulfate droplets). They suggest that in case the α-pdf scheme is used, it should be expressed as a function of water activity. In the study of Wheeler et al. (2014) it leads to good results for ATD, but less so for kaolinite. In both cases the best scheme was the active sites scheme, which was not investigated in the present study. In Welti et al. (2012) as well as in the present study the α-pdf scheme reproduces the data quite well. Note that this study, the study of Lüönd et al. (2010) and Welti et al. (2012) are the only studies where the size and time dependence has been tested separately (Crit. 2) as size and time resolved data was available. From the results presented here, we conclude that the α-pdf scheme is a suitable scheme to represent the time-dependence for kaolinite. This could explain why it achieves a better ranking here than in Wheeler et al. (2014) , where no size and time dependence could be tested against measurements. This paper includes the most complete evaluation (taking into account criterion 2 and 3 in addition to criterion 1) of contact angle schemes for immersion freezing of mineral dust types.

6 Conclusions

In this study the sensitivity of CNT based immersion freezing parameterization schemes to thermodynamic and kinetic parameters is investigated~~as a response to the large sensitivity of homogeneous freezing on these parameters .~~. We discuss their effect on the fit parameters of contact angle schemes when fitting measurement data. For the use in models ~~a validation of these~~ an assessment of sensitivities is important to estimate uncertainties ~~coming~~ originating from different parameterization schemes which ~~include~~ represent the effect of aerosol particles on the energy barrier of ice nucleation.

Compared to homogeneous freezing, immersion freezing has one more unconstrained parameter, namely the ~~contact angle α~~geometric term $f(\alpha)$. Different schemes to represent the contact angle ~~/-distribution~~ or contact angle distribution with one or two fit parameters based on experimental data are tested. It is found that ~~several different~~ contact angle schemes containing two fit parameters are able to reproduce ~~the experimental freezing curve. These schemes contain two fit parameter~~experimental FF , while the contact angle scheme with only one fit parameter, the single-α scheme, cannot reproduce the freezing curves.

Analyzing the importance of the choice of σ_{iw} and $\Delta g^{\#}$ to parameterize immersion freezing revealed that uncertainties in the thermodynamics or kinetics can be compensated by two-parameter contact angle schemes. As a result an under/overestimation of σ_{iw} ~~/~~or $\Delta g^{\#}$ does not lead to a bad representation of freezing curves as in case of homogeneous freezing. Because the fit parameters compensate inaccuracies or uncertainties of the thermodynamic and kinetic parameters, the absolute value of the found fit parameters is highly dependent on the choice of thermodynamic ~~/~~and kinetic parameters within the formulation of CNT (especially on σ_{iw}). As a consequence, contact angles for CNT parameterization schemes from different authors ~~can~~ should only be applied within the same CNT formulation ~~. Implementing one formulation of CNT~~ used to derive the parameters. Implementing a CNT based parameterization scheme into a GCM ~~together with a different estimate for α might introduce an offset into modeling studies (see red curve in Fig. 3). Besides the~~ demands that parameters derived from experiments are calculated using the same CNT formulation. Otherwise an offset of the freezing temperature in clouds might be introduced. The sensitivity of α on the thermodynamic and kinetic parameters used in CNT ~~makes~~ biases a direct comparison of contact angle values derived in different studies~~impossible. It again stresses~~. We emphasize the importance of highlighting which CNT formulation was used for the analysis of experimental data~~as stressed in Ickes et al. (2015) .~~.

~~Another consequence is that the reproducibility of freezing curves should not be the only criterion to decide on a CNT formulation because it can be misleading if the formulation has at least two fit parameters. Therefore some criteria to evaluate reasonable CNT formulations are compiled here. They additionally take into account the microphysical perspective (assumptions the CNT formulation is based on)~~ Contact angle schemes with two or more fit parameters reproduce freezing curves but can be unphysical or limited to the dataset used for fitting. Contact angle schemes intended to represent immersion freezing properties of a heterogeneous particle population under a variety of environmental conditions and time scales, should reproduce the T-dependence of freezing and the ability to predict the size and time dependence of the freezing process ~~.~~ (Crit. 1 and 2).

The schemes should be conform to the microphysical assumptions CNT is based on (Crit. 3). Particle size and nucleation time are implicitly included in the reproducibility of freezing curves of the dataset but should be ~~evaluated separately.~~ investigated separately. It should be noted here, that most experimental datasets are not accounting for both, the size and time dependence of freezing. Experimental data without any information on the time or size dependence limit the assessment according to the criteria defined in this study. Here only a full analysis of the CNT parameterization schemes for one mineral dust (kaolinite) was possible. Having limited datasets may lead to unrepresentative conclusions. More size and time dependent measurements of different IN are desirable to compile parameters and find a robust CNT formulation.

~~The fit parameters for scheme 2, scheme 5 and scheme 7 are determined~~ In this study we derived fit parameters for five different datasets of mineral dust (kaolinite Fluka, ~~NX illite~~illite-NX, montmorillonite, microcline and ATD) by fitting ~~the CNT approach~~ different CNT formulations to the FF from measurements. Good results in reproducing the freezing curves (~~criterion~~ Crit. 1: T-dependence and partly 2: size and time dependence) are achieved when using a single-α scheme with fitted constant $\Delta g^{\#}$ (CNT #2), an α-pdf scheme (CNT #5) or an α(T) scheme (CNT #7)~~when ignoring unreasonable solutions for the fit parameters (criterion 3). The single-α scheme does not perform well when $\Delta g^{\#}$ is not used as an additional fit parameter. The three good working CNT formulations (2, 5 and 7) are further evaluated by looking how well they reproduce the time and particle size dependence of the kaolinite dataset (criterion 2). In this case the α-pdf scheme (CNT 5) works better, as it captures the time dependence. However, the particle size dependence is underpredicted. Using a single-α scheme with fitted constant $\Delta g^{\#}$ (CNT 2) or an $\alpha(T)$ scheme (CNT 7) overpredicts the size and time dependence. Note that the results only refer to the kaolinite dataset. Due to this restriction it remains ambiguous which CNT formulation best fulfills criterion 2 and thus is best suited for modeling purpose. It would be helpful to redo the analysis for other dust types. From the perspective of criterion 2 all three CNT formulations seem to be able to predict nucleation rates for mineral dust particles. An empirical immersion freezing parameterization scheme based on Niemand et al. (2012) can also capture the freezing curves and IN size dependence quite well. However, it is not clear if it is legitimate to extrapolate the empirical relationship, so that the full T-range is covered. Criterion 3 is difficult to evaluate coming from a macroscopic level as microphysical knowledge is missing at this point. Scheme 5 is consistent with the microphysical perspective of freezing. Evaluating scheme 2 requires knowledge about a possible influence on $\Delta g^{\#}$ by an aerosol particle immersed in the supercooled droplet and is thus not possible. Scheme 7 can return unphysical fit parameters (criterion 3 is not always fulfilled). However, this evaluation is limited by the recognition how α might change with temperature.~~

~~More size and time dependent measurements of different IN would be beneficial to evaluate different CNT formulations more robustly.~~

.

Table 1. List of symbols

Symbol	Unit	Description
A_{IN}	m^2	Surface area of an IN
A_{tot} ~~,~~	m^{-2}	Total surface area per unit volume of particles over all size bins
$A_{\text{tot},j}$	m^{-2}	Total surface area per unit volume of particles in size bin j
A_j	m^{-2}	Dust particle surface area in size bin j
~~$C_{\text{prefac,hom}}$~~ C_{prefac}	$\text{m}^{-3}\ \text{s}^{-1}$	Preexponential factor of the ~~homogeneous~~ nucleation rate
d	m	Aerosol particle diameter
f	-	Geometric term
f_{mean}	-	Mean geometric term of the contact angle distribution
f_{260}, f_{250}, f_{240}	-	Geometric term at T=260, 250 or 240 K
FF	-	Frozen fraction
h	J s	Planck constant
J_{hom}	$\text{m}^{-3}\ \text{s}^{-1}$	Homogeneous nucleation rate
J_{imm}	$\text{m}^{-2}\ \text{s}^{-1}$	Immersion freezing nucleation rate
k_{B}	J K^{-1}	Boltzmann constant
$n_{k,\text{germ}}$	-	Number of water molecules in the ice germ
n_{s}	m^{-2}	Number of water molecules in contact with the unit area of the ice germ
$n_{\text{s,IN}}$	m^{-2}	Surface density of active sites on an IN
N_{i}	-	Ice crystal number concentration
$N_{\text{i,j}}$	-	Number of ice active aerosol particles in size bin j
N_{l}	m^{-3}	Volume number density of a water molecule in liquid water
$N_{\text{tot,j}}$	-	Total number of aerosol particles in the size bin j
m	rad K^{-1}	Change of contact angle with temperature
$p(\alpha)$	-	Probability density of contact angle α
r_{germ}	m	Radius of the ice germ (=critical radius)
r_{IN}	m	Radius of the IN
S_{i}	-	Saturation ratio with respect to ice
t	s	Time
T	K	Temperature
v_{ice}	m^3	Volume of a water molecule in the ice embryo
Z	-	Zeldovich factor
α	rad	Contact angle
α_0	rad	Contact angle at melting point
$\Delta g^{\#}$	J	Activation energy barrier
ΔG,ΔG_{hom}	J	Gibbs free energy barrier (of homogeneous freezing)
Δt	s	Time step
μ	~~rad~~ -	~~Mean~~ Natural logarithm of the mean contact angle of the contact angle distribution
σ	-	Variance of the contact angle distribution
σ_{iw}	J m^{-2}	Interfacial tension between ice/water
π	-	Ratio of a circle's circumference to its diameter

Table 2. Overview of CNT formulations used for the sensitivity analysis, results for the fit parameters and evaluation of the fit result. The values are rounded to two digits after the decimal point. The logarithmic mean contact angle μ and the temperature dependent contact angles are converted into the corresponding geometric term f using Eq. 3.

CNT formulation #1, #5 and #7 use the best fitting combination of σ_{iw} and $\Delta g^{\#}$ emerging from the homogeneous freezing analysis in Ickes et al. (2015).

#	~~**Formulation**~~ **Parameterization for** σ_{iw} **and** $\Delta g^{\#}$	**Contact angle**~~**scheme**~~ **scheme**	**Name**	**Fit parameters**	RM
1	σ_{iw}: Reinhardt and Doye (2013) $\Delta g^{\#}$: Zobrist et al. (2007)$\approx 5\cdot 10^{-20}$J	single-α	Single-α R&D + Z	1: f=0.55	0.12
2	σ_{iw}: Reinhardt and Doye (2013) $\Delta g^{\#}$: constant	single-α	Single-α R&D + fit $\Delta g^{\#}$	2: f=0.24 $\Delta g^{\#}$=11.01$\cdot 10^{-20}$J	0.05
3	σ_{iw} from Ouchi (1954) $\Delta g^{\#}$: constant	single-α	Single-α O + fit $\Delta g^{\#}$	2: f=0.69 $\Delta g^{\#}$=12.3$\cdot 10^{-20}$J	0.05
4	σ_{iw} from Eadie (1971) $\Delta g^{\#}$: constant	single-α	Single-α E + fit $\Delta g^{\#}$	2: f=0.23 $\Delta g^{\#}$=10.46$\cdot 10^{-20}$J	0.05
2/4	σ_{iw}: Reinhardt and Doye (2013) $\Delta g^{\#}$: constant	single-α	Single-α R&D + fit $\Delta g^{\#}$(E)	2: f=0.24 (#2) $\Delta g^{\#}$=10.46$\cdot 10^{-20}$J (#4)	0.31
5	same as #1	α-pdf	α-pdf R&D + Z	2: μ=0.5 ~~rad~~ $\Rightarrow \alpha_{\mathrm{mean}}$=94.46° $\hat{=}\ f_{\mathrm{mean}} \approx$0.56 σ=0.04	0.05
6	σ_{iw} from Eadie (1971) $\Delta g^{\#}$: Zobrist et al. (2007)	α-pdf	α-pdf E + Z	2: μ=0.44 ~~rad~~ $\Rightarrow \alpha_{\mathrm{mean}}$=88.96° $\hat{=}\ f_{\mathrm{mean}} \approx$0.48 σ=0.03	0.05
7	same as #1	$\alpha(T)$	$\alpha(T)$ R&D + Z	2: α_0=0.7 rad=40.1° $\hat{=}\ f_{260} \approx$0.18 $f_{250} \approx$0.37 $f_{240} \approx$0.59 m= -0.03 rad K^{-1}	0.05

Table 3. ~~Estimated~~ Derived fit parameters for the different CNT formulations ~~used for~~ and five different mineral dust types [kaolinite (kao), illite (ill), montmorillonite (mont), microcline (micro), ATD]. The values are rounded to two digits after the decimal point. The logarithmic mean contact angle μ and the temperature dependent contact angles are converted into the geometric term f using Eq. 3.

#	**Fit parameter**	Kao	RMSE	Ill	RMSE	Mont	RMSE	Micro	RMSE
1	f	0.56	0.2	0.61	0.17	0.56	0.18	0.3	0.22
2	f	0.29	0.14	0.36	0.14	0.28	0.09	0.11	0.1
	$\Delta g^{\#}/10^{-20}$ J	9.95		8.93		10.03		11.97	
5	μ ~~/rad~~	0.5	0.09	0.54	0.13	0.5	0.15	0.25	0.13
	$\hat{=}\, f_{mean}$	≈ 0.56		≈ 0.61		≈ 0.56		≈ 0.29	
	σ	0.06		0.05		0.04		0.11	
7	α_0/rad	0.84	0.14	0.98	0.13	0.81	0.09	0.61	0.1
	$\hat{=}\, f_{260}$	≈ 0.18		≈ 0.27		≈ 0.17		≈ 0.14	
	$\hat{=}\, f_{250}$	≈ 0.31		≈ 0.4		≈ 0.29		≈ 0.31	
	$\hat{=}\, f_{240}$	≈ 0.45		≈ 0.55		≈ 0.43		≈ 0.53	
	$m/(\mathrm{rad\ K^{-1}})$	-0.02		-0.02		-0.02		-0.03	

#	**Fit parameter**	ATD	RMSE
1	f	0.58	0.32
2	f	0.14	0.21
	$\Delta g^{\#}/10^{-20}$ J	12.58	
5	μ ~~/rad~~	0.48	0.25
	$\hat{=}\, f_{mean}$	≈ 0.54	
	σ	0.16	
7	α_0/rad	0.39	0.13
	$\hat{=}\, f_{260}$	≈ 0.1	
	$\hat{=}\, f_{250}$	≈ 0.31	
	$\hat{=}\, f_{240}$	≈ 0.61	
	m	-0.04	

Table 4. Ranking of the capability of the different CNT formulations to reproduce the freezing curves for different mineral dust particles based on the RMSE between the calculated freezing curve and the measured freezing data.

#	Kaolinite	Illite	Montmorillonite	Microcline	ATD	Average ~~score~~ ranking
1	3	3	3	3	4	3.2
2	2	2	1	1	2	1.6
5	1	1	2	2	3	1.8
7	2	1	1	1	1	1.2

#	Average RMSE	~~Score~~ Ranking based on average RMSE
1	0.218	4
2	0.136	2
5	0.15	3
7	0.118	1

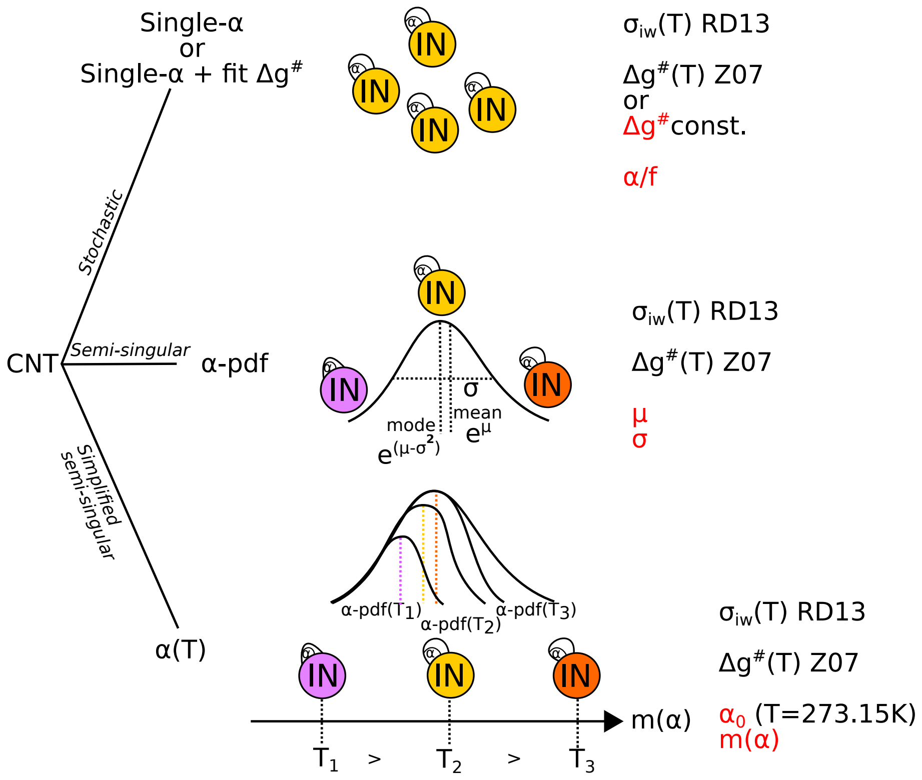

Figure 1. Schematic sketch of different contact angle schemes in which the fit parameters for each contact angle scheme are marked in red.

Stochastic: ~~all~~ All IN ~~contain~~ have the same contact angle α (single-α). The ice germ ~~including~~ with the contact angle α is shown in the sketch.

Semi-singular: Different IN ~~contain~~ have different contact ~~angle α, but each IN has a single α~~angles. The contact angles are distributed with an α-pdf over the IN population. The sketch shows three ~~different~~ contact angles α_1 (~~orange~~purple), α_2 (yellow) and α_3 (~~purple~~orange) of the contact angle distribution. The ~~least~~ most efficient contact angle α_1 is the ~~largest~~ smallest (~~$> \alpha_2 > \alpha_3$~~$< \alpha_2 < \alpha_3$).

Simplified semi-singular: All IN ~~contain a singular~~ have the same contact angle~~with $\alpha_1 > \alpha_2 > \alpha_3$ shown as an example~~. The contact angle changes with T ($\alpha_1 < \alpha_2 < \alpha_3$ in the example). α is equivalent to the mean contact angle ~~μ~~ of the α-pdf scheme (e$^{\mu}$) or mean activity of the α-pdf distribution, which changes with temperature~~in analogon to the time/temperature evolution of the α-pdf α(T). The fit parameters for each contact angle scheme are marked in red~~. Figure adapted from F. Lüönd.

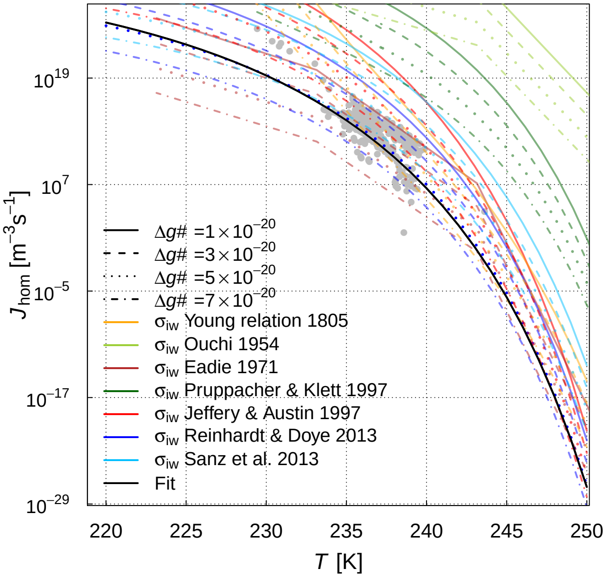

Figure 2. Comparison of the fitted $J_{\rm hom}(T)$ (solid black line) with calculated nucleation rates using different formulations of $\sigma_{\rm iw}$ and constant values for $\Delta g^{\#}$. Grey dots show ~~the collected~~ experimental homogeneous freezing ~~dataset~~data. $\sigma_{\rm iw}$ from Reinhardt and Doye (2013) captures the homogeneous freezing curve ~~the~~ best.

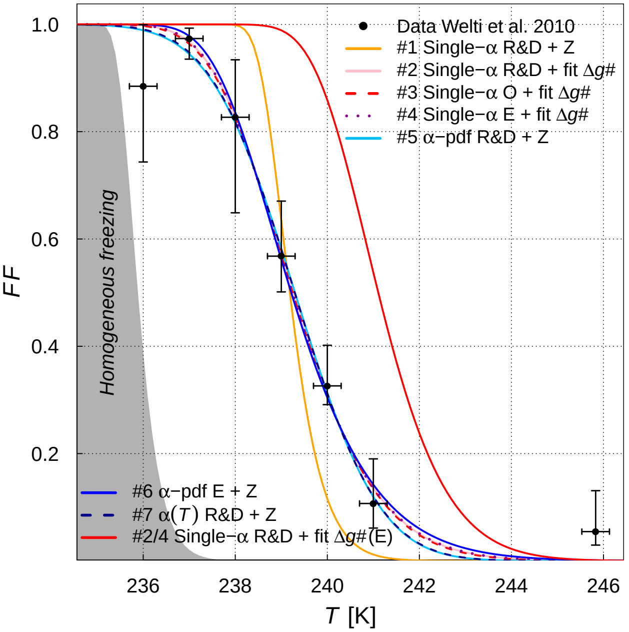

Figure 3. Calculated frozen fraction FF as a function of T for different thermodynamic and kinetic parameters in combination with different contact angle schemes for kaolinite with a particle diameter of 400 nm after a residence time of 10 s. More details can be found in Table 2.

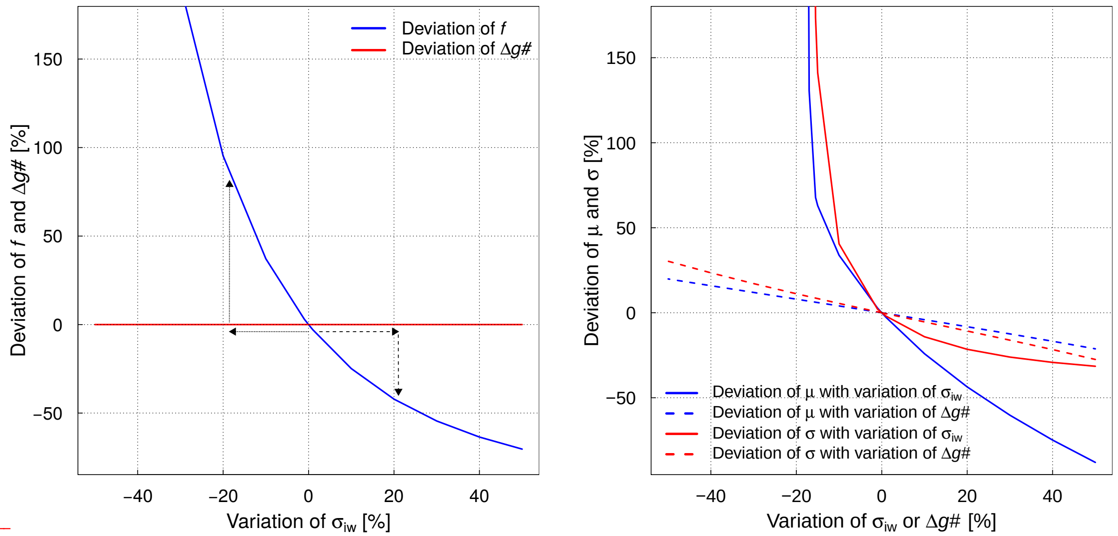

(a) Sensitivity analysis for the single-α R&D + fit $\Delta g^{\#}$ formulation (CNT #2)

(b) Sensitivity analysis for the α-pdf R&D + Z formulation (CNT #5)

Figure 4. Magnitude of deviation from a reference fit in percent (relative uncertainty) ~~. The results are shown for~~ due to a variation of σ_{iw} and $\Delta g^{\#}$ from 0 to ± 50%. The applied change is indicated by the line type ~~(~~[solid = change in thermodynamics (σ_{iw}), dashed = change in kinetics ($\Delta g^{\#}$)~~. The figure can be used to estimate the direction in which fit parameters deviate~~].

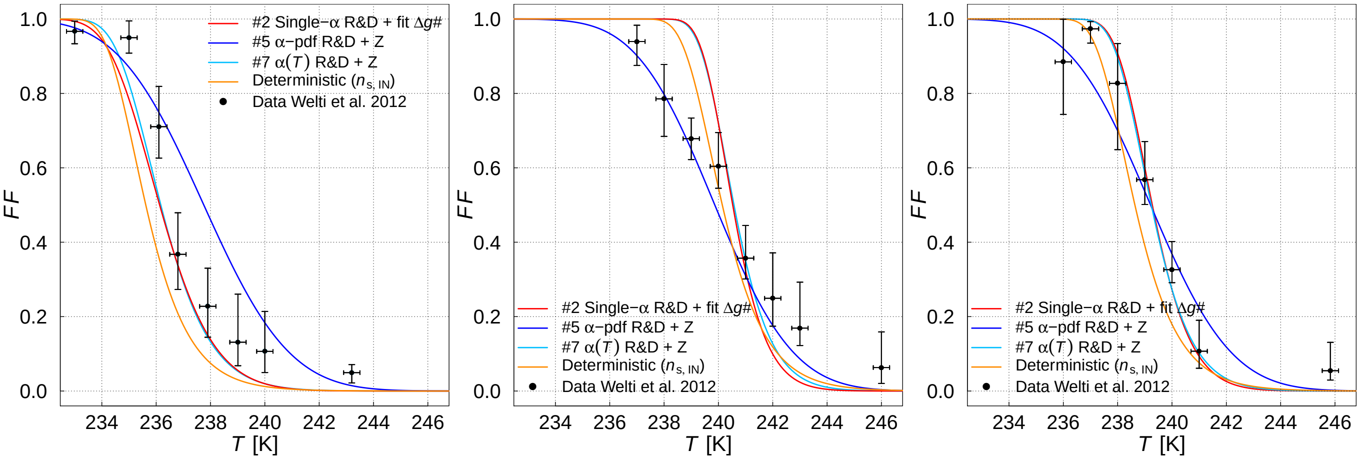

(a) d=100 nm, t=10 s

(b) d=800 nm, t=10 s

(c) d=400 nm, t=10 s

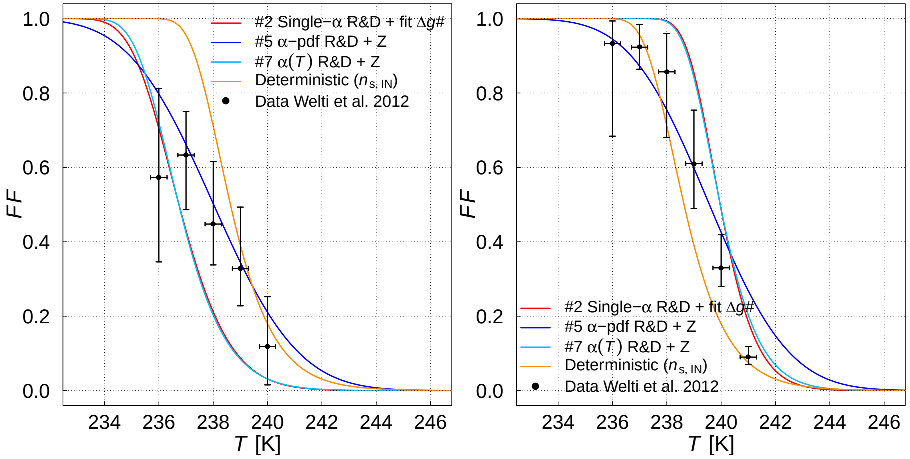

(d) d=400 nm, t=1 s

(e) d=400 nm, t=21 s

Figure 5. Calculated FF of kaolinite for ~~certain~~ three different times and three sizes using the single-α R&D + fit $\Delta g^{\#}$ ~~scheme~~ formulation (CNT #2), the α-pdf R&D + Z ~~scheme~~ formulation (CNT #5) and the $\alpha(T)$ R&D + Z ~~scheme~~ formulation (CNT #7) with corresponding fit parameters (see Table 3) and a simplified immersion freezing parameterization scheme based on Niemand et al. (2012) compared to the dataset. ~~Figure~~ (a)-(c) show the particle size dependence (t=10 s), ~~Fig.~~ (c)-(e) show the time dependence (d=400 nm).

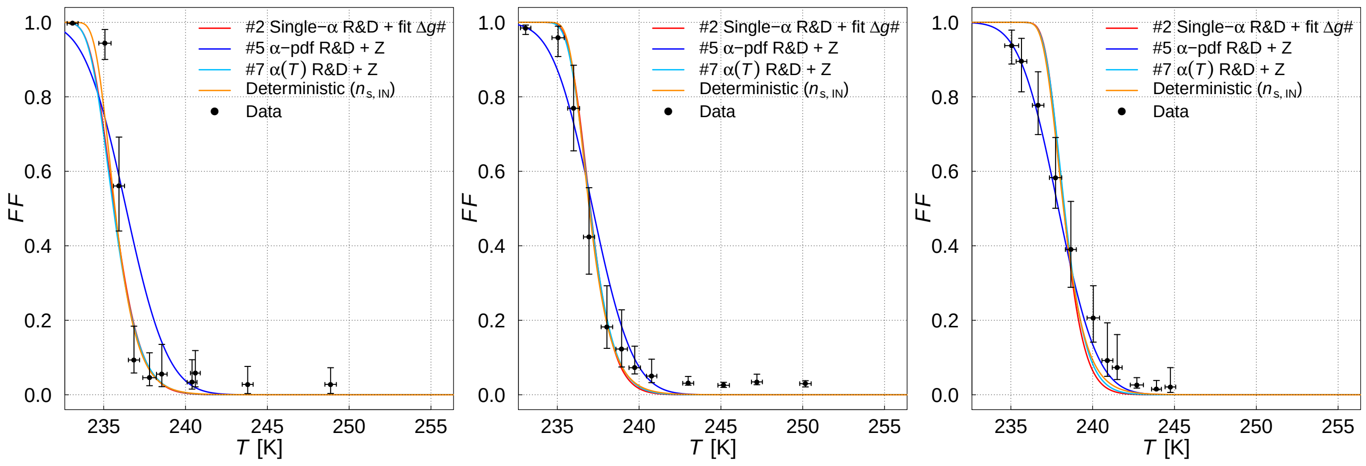

(a) Illite, d=100 nm

(b) Illite, d=200 nm

(c) Illite, d=400 nm

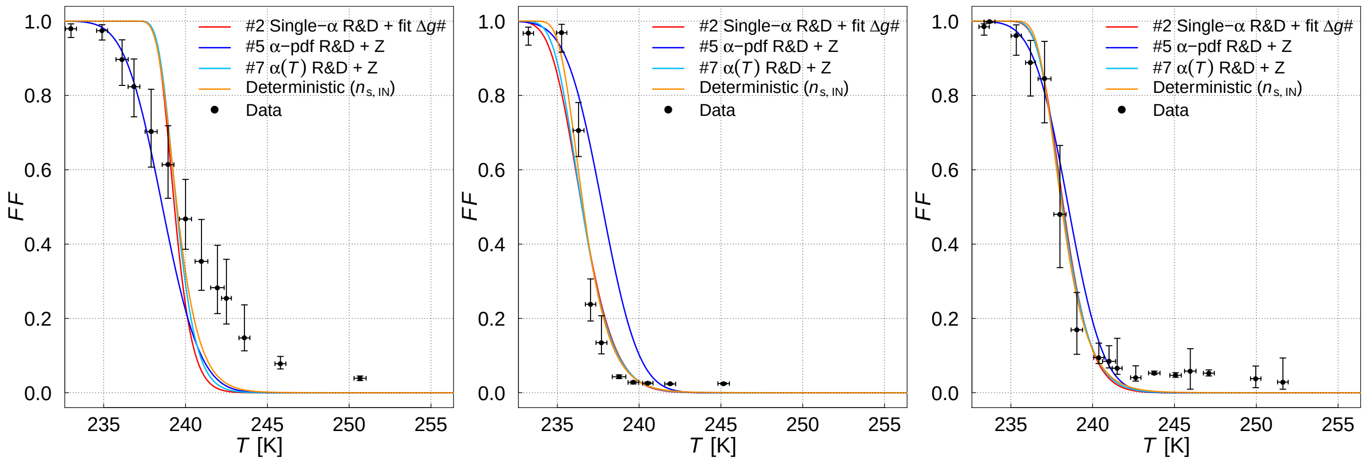

(d) Illite, d=800 nm

(e) Montmorillonite, d=100 nm

(f) Montmorillonite, d=200 nm

Figure 6. Calculated FF of illite [(a)-(d)], montmorillonite [(e)-(h)], microcline [(i)-(m)] and ATD [(n)-(q)] after a residence time t of 10 s for certain sizes using the single-α R&D + fit $\Delta g^{\#}$ ~~scheme~~ formulation (CNT #2), the α-pdf R&D + Z ~~scheme~~ formulation (CNT #5) and the $\alpha(T)$ R&D + Z ~~scheme~~ formulation (CNT #7) with corresponding fit parameters (see Table 3)~~and a~~. A simplified immersion freezing parameterization scheme based on Niemand et al. (2012) is additionally compared to the dataset.

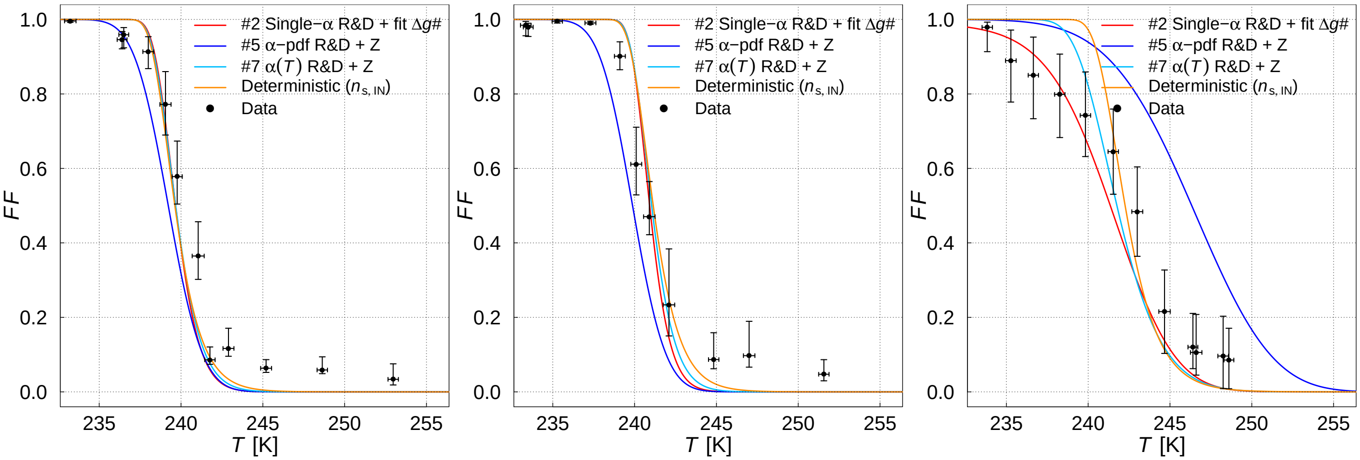

(g) Montmorillonite, d=400 nm (h) Montmorillonite, d=800 nm (i) Microcline, d=50 nm

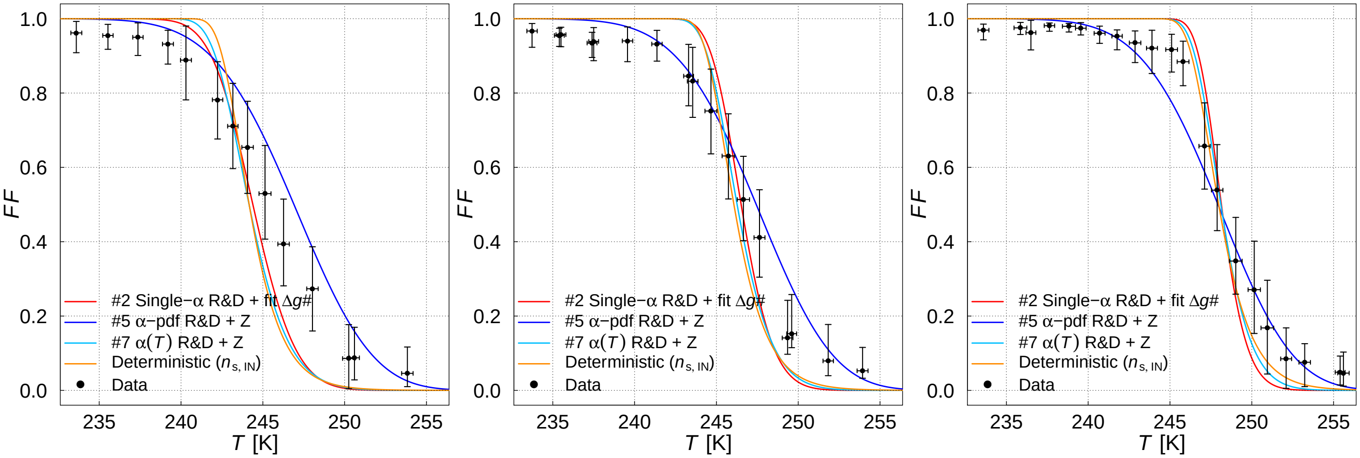

(j) Microcline, d=100 nm (k) Microcline, d=200 nm (l) Microcline, d=400 nm

Figure 6. Continued.

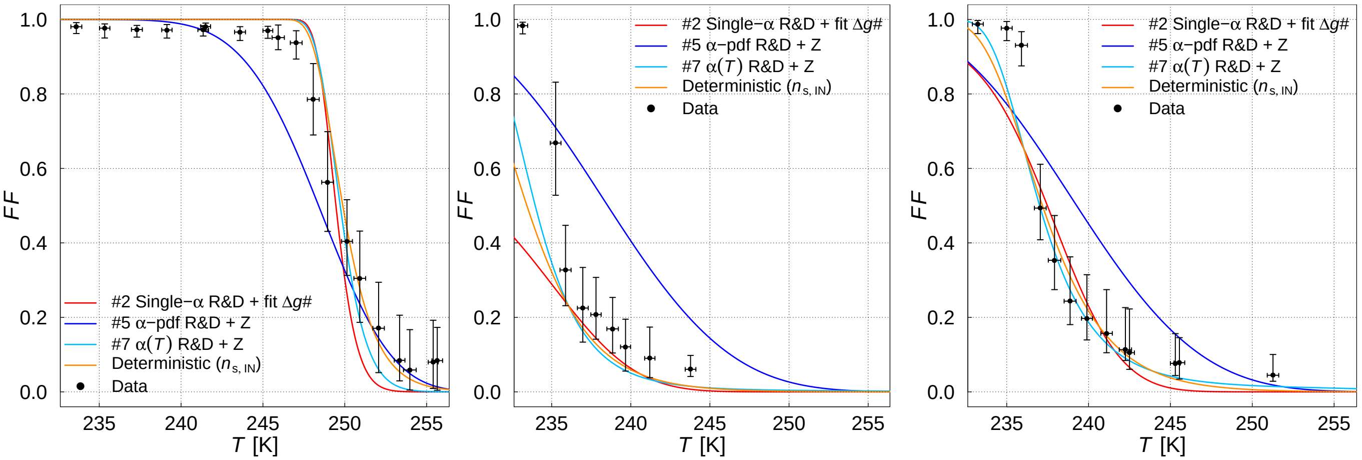

(m) Microcline, d=800 nm

(n) ATD, d=100 nm

(o) ATD, d=200 nm

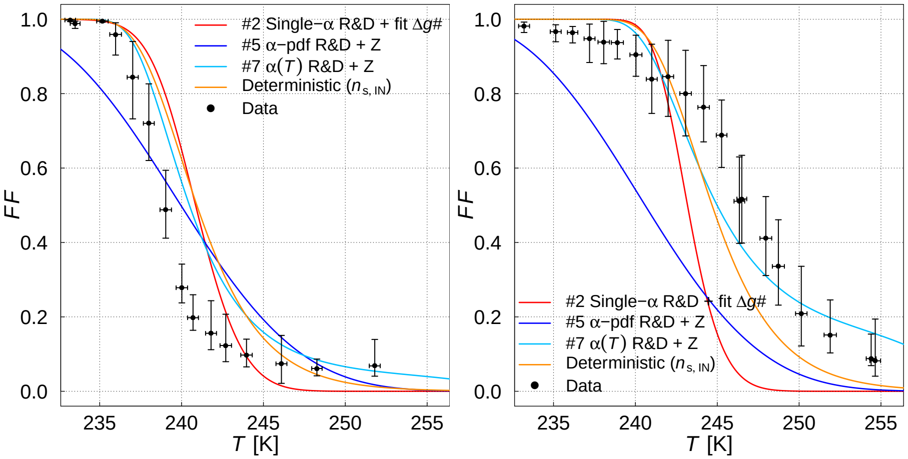

(p) ATD, d=400 nm

(q) ATD, d=800 nm

Figure 6. Continued.

Appendix A: Analysis of the different contact angle scheme formulations: How ~~do~~ the fit parameters influence the calculated nucleation rate/frozen fraction

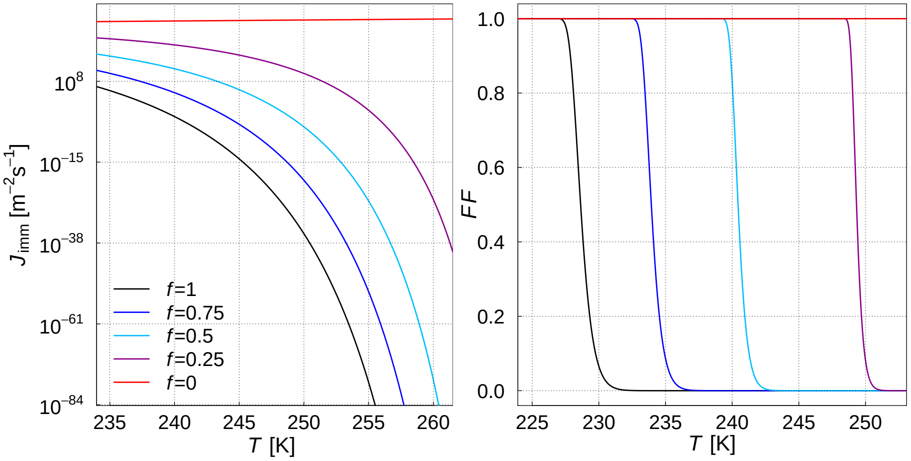

(a) CNT #1: J_{imm} in dependence of f

(b) CNT #1: FF in dependence of f

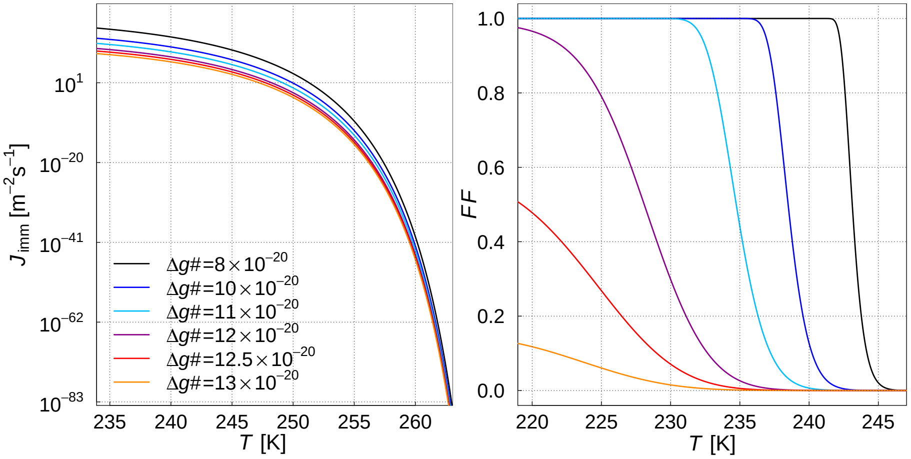

(c) CNT #2: J_{imm} in dependence of $\Delta g^{\#}$

(d) CNT #2: FF in dependence of $\Delta g^{\#}$

Figure 7. Nucleation rate J_{imm} and frozen fraction FF in dependence of the fit parameters for the ~~different contact-angle~~ contact angle schemes #1 and #2 (~~here~~ f and $\Delta g^{\#}$). To estimate FF we assume an aerosol particle diameter of 400 nm and a timestep of 10 s. In case of the single-α R&D + fit $\Delta g^{\#}$ scheme (#2) the geometric term f was chosen to be ~~0.4~~0.3. ~~Note that the~~ The dependence of the ~~scheme~~ formulation (in the case of a fixed $\Delta g^{\#}$) on f is the same as with the single-α R&D + Z ~~scheme~~ formulation (#1).
Decreasing f (reducing the energy barrier) shifts the freezing curve to ~~warmer~~ higher temperatures ~~. The~~ while the slope ~~changes only negligible~~slightly increases. Increasing $\Delta g^{\#}$ ~~(increasing the activation energy barrier)~~ shifts the freezing curve to lower temperatures ~~. It also~~ and changes the slope of the ~~curve. a~~ freezing curve. A higher activation energy barrier leads to a flattening of the curve.

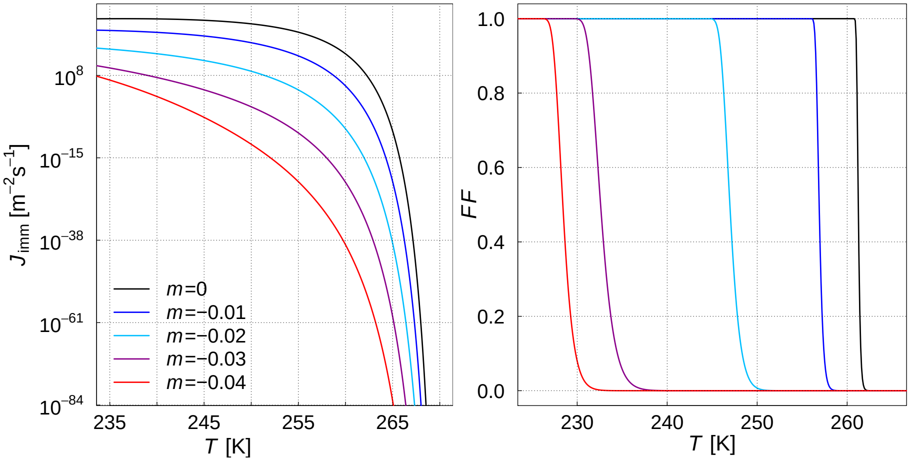

(a) CNT #7: J_{imm} in dependence of m

(b) CNT #7: FF in dependence of m

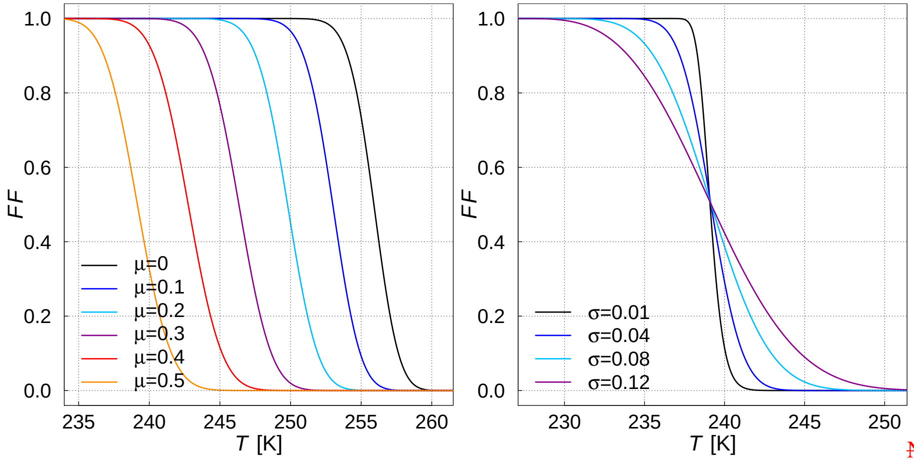

(c) CNT #5: FF in dependence of μ

(d) CNT #5: FF in dependence of σ

~~Nucleation rate J_{imm} and frozen fraction FF in dependence of the fit parameters for the different contact-angle schemes (here m, μ and σ). In case of scheme 7 α_0 was chosen to be 1.5 (≈ 85°). Note that the dependence of the scheme (in the case of a fixed change in contact angle m) on α_0 is the same as the change with f of the single-α RD + Z scheme (1). In case of the α-pdf RD + Z scheme (5) σ was chosen to be 0.01 in the left figure, μ was chosen to be 0.3 (≈ 18°) in the right figure. Decreasing m (contact angle gets larger with T because most efficient IN are used first) shifts the freezing curve to colder temperatures and changes the slope of the curve (flattening). Increasing μ (increasing the contact angle) shifts the freezing curve to lower temperatures and flattens the curve, while an increase in σ (broadening of the contact angle distribution) changes the slope of the freezing curve only (flattening). Note that already small changes in μ lead to a considerable shift of the curve compared to the other schemes.~~

Figure 8. Nucleation rate J_{imm} and frozen fraction FF in dependence of the fit parameters for the contact angle schemes #7 and #5 (m, μ and σ). To estimate FF we assume a aerosol particle diameter of 400 nm and a timestep of 10 s. In case of CNT #7 α_0 was chosen to be 0.8 (≈ 46°). Note that the dependence of the scheme on α_0 (in the case of a fixed change in contact angle m) is the same as the change with f of the single-α R&D + Z formulation (CNT #1). In case of the α-pdf R&D + Z formulation (CNT #5) σ was chosen to be 0.05 in the left figure, μ was chosen to be 0.5 (≈ 29°) in the right figure.

Decreasing m (increasing contact angle with decreasing T because a broader part of the IN populations contact angle distribution causes nucleation) shifts the freezing curve to lower temperatures and changes the slope of the curve (flattening).

Increasing μ (increasing the average contact angle) shifts the freezing curve to lower temperatures and slightly flattens the curve, while an

Appendix B: Estimating the relative uncertainty of fitting α: Example calculations

Figure 4 can be used to estimate the deviation of fit parameters from different CNT formulations relative to each other. To show this, we estimate the difference in fit parameter when using σ_{iw} from Eadie (1971) instead of Reinhardt and Doye (2013) in combination with an α-pdf scheme ~~scheme (~~(CNT #6 ~~) compared to scheme (~~compared to CNT #5). Within the 10 K temperature range of the immersion freezing measurements (236-246 K) σ_{iw} is on average 4% higher when using σ_{iw} from Eadie (1971) instead of Reinhardt and Doye (2013). ~~An~~ From Fig. 4 b we see that an increase in σ_{iw} by 2.5% (246 K) or 5% (236 K) would lead to a decrease in μ by approximately 7 to 13%~~(see Fig. 4 b).~~. Now we check if that estimated change matches with the real change when fitting the same dataset with the two different σ_{iw}. In Table 2 using σ_{iw} from Eadie (1971) leads to a mean contact angle of 0.44 rad (approx. 25.5°) instead of 0.5 rad (approx. 28°) when using σ_{iw} from Reinhardt and Doye (2013). This is a difference of 12%, conform with the estimate from Fig. 4 (approx. 7-13%). However, the variance σ of the α-pdf distribution is expected to change less (5 to 9%) but a change by 25% is found ~~.~~ for the best fit.

In some cases the predicted change in fit parameters from Fig. 4 deviates from the real change in fit parameters (Table 2) ~~.~~ ~~The~~ because both parameter μ and σ are changed at the same time. For Fig. 4 one was held constant. Another problem with Fig. 4 is, that the assumption of a constant variation of σ_{iw} over the whole temperature range is invalid in most cases~~, so that~~. However, Fig. 4 can ~~not be used easily. However, it can~~ be used to illustrate how fit results might change and estimate a rough deviation from the reference when using different thermodynamic and kinetic parameters especially for cases where σ_{iw} changes nearly constant over the fitted temperature range. This can help when comparing fit results to fit results from ~~another study~~ studies where a different formulation of CNT was used.

Appendix C: Variability of the fit parameters throughout one dataset

The variability of the fit parameters throughout the dataset can be seen when fitting the single-α R&D + fit $\Delta g^{\#}$ ~~scheme (~~formulation (CNT #2)~~and~~, the α-pdf R&D + Z ~~scheme (~~formulation (CNT #5) and the $\alpha(T)$ R&D + Z formulation (CNT #7) to FF of kaolinite data for different sizes and residence times separately. The resulting fit parameters are compared in Fig. 9 for different sizes in red and for different times in blue and light blue. Each point in Fig. 9 represents the value of the best fit parameter for one subset of the kaolinite dataset. The labels on the x-axis give information which subset of the dataset was fitted. The residence time is 10 s for the data subsets of different sizes and the diameter of the kaolinite particles 400 nm or 800 nm for the data subsets of different times (blue/light blue). The dashed line indicates the mean of the size or time dependent fit parameter. The ~~standard deviation~~ range is shown as shaded box.

The fit parameters vary depending on the measurement conditions. Omitting the measurement with the ~~smallest aerosol particle size (d=100 nm) and the~~ shortest residence time (1 s) the variation between the data subsets for different times is small. The variability of the fit parameters is larger for different aerosol particle sizes compared to different residence times, which might be due to the higher sensitivity of the freezing process to particle size compared to time. ~~For scheme~~ For CNT #2 the fit parameters seem to be correlated. High values of one fit parameter, e.g. f, correspond to low values of the other fit parameter, e.g. $\Delta g^{\#}$. ~~Scheme~~ CNT #5 on the other hand does not show a clear correlation ~~.~~ for the time dependent subsets, but for the size dependent subsets. The same yields for CNT #7.

The different fit results for ~~scheme~~ CNT #5 can be used to study how the shape of the contact angle distribution might change with the size of the particles or the residence time.

Whereas the fitted contact angle distribution does not change noticeable with time between 1 and 21 s (Figure not shown here), the mean contact angle (e^{μ}) and the variance σ changes with particle size (see Fig. 10). ~~The~~ For all mineral dust types investigated here the contact angle distribution is shifted to the left (smaller contact angles) with increasing size, which means that the mean freezing efficiency of the IN population increases with size. Additionally for all mineral dust types except microcline the contact angle distribution broadens with increasing aerosol particle size (neglecting the fit of the 400 nm dataset of kaolinite, which does not fit into the picture)~~, which~~. This reflects a larger probability of different α on the aerosol particle population with increasing size. The particle population is more heterogeneous. ~~Additionally the maximum is shifting to the left (smaller contact angle) which means that the IN is getting more efficient~~ In the case of microcline the contact angle distribution narrows with increasing aerosol particle size, the ice nucleating properties of the microcline aerosol population seem to get more homogeneous with size. Note that the curves (here shown for kaolinite and microcline) are not considering measurement uncertainties of the fitted data and therefore can only be used to qualitatively interpret the result. In case of idealized measurements the result could be used to derive a relationship ~~for~~ between mean contact angle (e^{μ}) or the width of the contact angle distribution σ and the size of the IN. Using the results of Fig. 9 and developing a size-dependent α-pdf improves the fit results.

C1 Uncertainty of fit parameters due to limited data

In many cases ~~there are not~~ no size- and time-dependent measurements are available. Here we investigate the quality of fit parameters if only limited amount of data is available. For that purpose we use the kaolinite dataset (as this is the most ~~thoroughly~~ extensive dataset available within this study) and use only subsets of the dataset ~~assuming that not all data is available~~ to estimate the fit parameters. The quality of the gained fit parameters is then estimated by using the complete dataset and look how good the freezing curves can be represented (RMSE). We look at four different cases:

1. Reference, the whole dataset is fitted (see also Table 3).
2. Only size dependent measurements are available, time dependence is not known (t=10 s).
3. Only time dependent measurements are available, size dependence is not known (d=400 nm).
4. Only one measurement is available (t=10 s, d=400 nm).

The resulting fit parameters and the deviation from the entire kaolinite dataset is shown in Table 5. The fit parameters are not significantly different when the dataset is limited to only size or only time dependent data. Also the deviation from the complete dataset is not significant~~(RMSE)~~. This analysis therefore does not allow any conclusion how many dependencies, e.g. size and time, have to be taken into account to successfully fit freezing ~~curves. However~~data. However, if using only one single dataset, the results for the fit parameters are different and the deviation from the measurements is higher. Note that the deviation when fitting only a single dataset could be larger if a dataset is chosen which is not similar to the average values of the dataset as in this case. This means that there is no guarantee that fits can be extrapolated/used in a universal way across different conditions.

~~Estimated~~

Table 5. Derived fit parameters for ~~the~~ two different CNT formulations ~~used for kaolinite using~~ based on the complete kaolinite dataset or subsets of the ~~dataset~~data. The values are rounded to two digits after the decimal point. The RMSE value ~~shows~~ is the deviation of the fit to the complete dataset.

#	**Fit parameter**	~~Reference~~ All data	RMSE	Only size	RMSE	Only time	RMSE	Only one dataset	RMSE
2	f	0.29	0.14	0.29	0.14	0.3	0.14	0.23	0.15
	$\Delta g^{\#}/10^{-20}$ J	9.95		9.93		9.7		11.01	
5	μ ~~/rad~~	0.5	0.09	0.5	0.1	0.5	0.09	0.49	0.12
	σ	0.06		0.05		0.07		0.04	

~~Change of α-pdf with particle size for the kaolinite dataset. The residence time is 10 s.~~

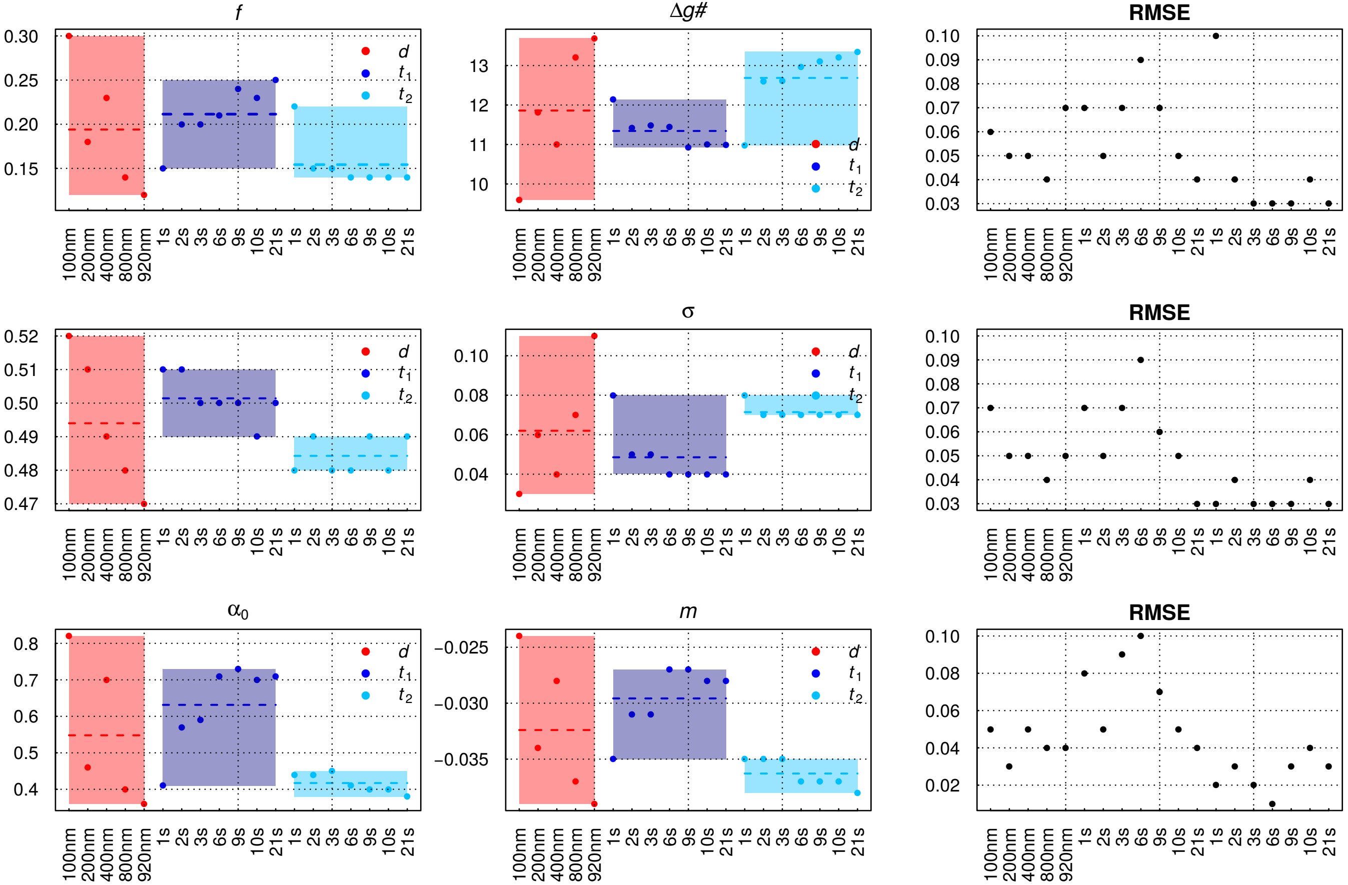

Figure 9. Variability of the fit parameters ~~throughout~~ for subsets of the kaolinite dataset. The variability with the aerosol particle size (d) is shown for a residence time t of 10 s (red). The variability with ~~the~~ time (t_1 and t_2) is shown for a aerosol particle diameter of 400 nm (t_1, blue) and 800 nm (t_2, ~~lightblue~~light blue). The first row shows the fit results for ~~scheme~~ CNT #2, the second row for ~~scheme~~ CNT #~~5.~~ 5, the third row for CNT #7. The RMSE value shows the deviation of the fit to the single dataset it was fitted to.

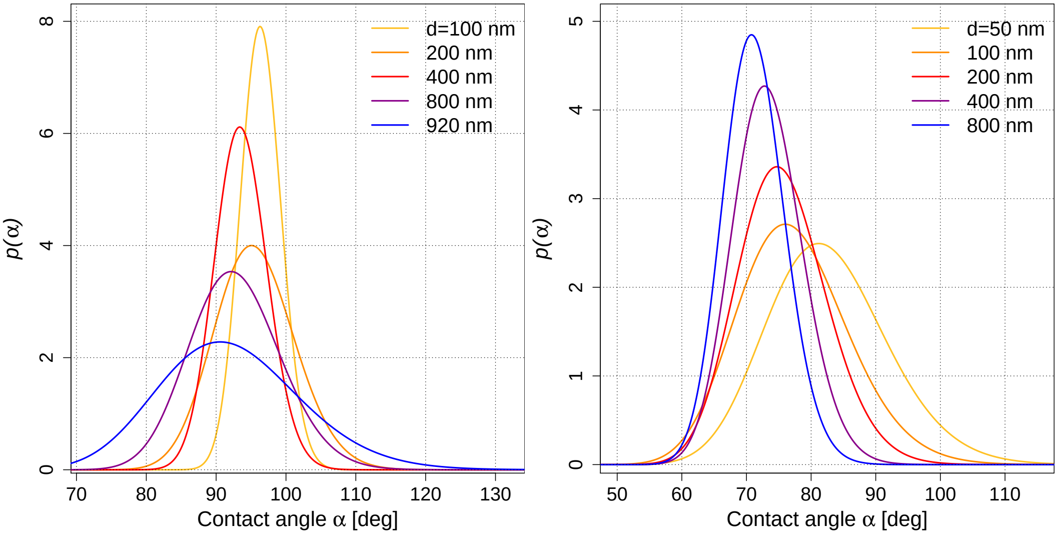

(a) Kaolinite

(b) Microcline

Figure 10. Change of α-pdf with particle size for the kaolinite and microcline dataset. The residence time is 10 s.

Appendix D: Estimating the surface site density $n_{\mathrm{s,IN}}$

The Niemand et al. (2012) scheme for immersion freezing of natural dust ~~,~~ is a deterministic scheme based on the approach of Connolly et al. (2009). It is derived from measurements carried out at the “Aerosol Interaction and Dynamics in the Atmosphere” (AIDA) cloud chamber at KIT, Karlsruhe ~~. A~~ [a detailed description of the AIDA cloud chamber and the measurements can be found in Niemand et al. (2012)~~.~~]. In this approach it is assumed that ice nucleation ~~is~~ occurs on localized sites, called active sites. It is described as a function of T and particle surface area A_{IN} because the amount of active sites ~~scales~~ is supposed to scale with particle size.

In Connolly et al. (2009) the change of the number of ice active aerosol particles in the size bin j, $N_{\mathrm{i},j}$, with respect to T is:

$$\frac{dN_{\mathrm{i},j}}{dT} = (N_{\mathrm{i},j} - N_{\mathrm{tot},j}) \cdot A_j \cdot k(T)\ , \tag{D1}$$

where $N_{\mathrm{tot},j}$ denotes the total number of aerosol particles in the size bin j and A_j ~~for~~ the dust particle surface area in the same size bin. The surface site density of ice active sites $n_{\mathrm{s,IN}}$ as a function of T can be determined by integrating the factor $k(T)$ over the whole temperature range:

$$n_{\mathrm{s,IN}}(T) = \int_T^0 k(T)dT\ . \tag{D2}$$

Using Eq. D1 and D2 the frozen fraction FF can be expressed as a function of T:

$$FF = \frac{N_{\mathrm{i},j}}{N_{\mathrm{tot},j}} = 1 - \exp(-A_j \cdot n_{\mathrm{s,IN}}(T)) \approx A_j \cdot n_{\mathrm{s,IN}}(T)\ . \tag{D3}$$

The approximation is valid for $A_j \cdot n_{\mathrm{s,IN}}(T) \ll 1$, which translates into small particles and high temperatures. For low temperatures, e.g. 243.15 K and particles larger than 3 μm the term $A_j \cdot n_{\mathrm{s,IN}}$ is approximately 1.
The surface site density of ice active sites, $n_{\mathrm{s,IN}}(T)$, is calculated from the total surface area of aerosol particles in the AIDA chamber and the measured ice crystal number concentration during one freezing experiment:

$$\begin{aligned}
\sum_{j=1}^{n} N_{\mathrm{i},j} \quad &\approx \quad \sum_{j=1}^{n} N_{\mathrm{tot},j} \cdot A_j \cdot n_{\mathrm{s,IN}}(T) = n_{\mathrm{s,IN}}(T) \cdot \sum_{j=1}^{n} N_{\mathrm{tot},j} \cdot A_j && \text{(D4)}\\
\Leftrightarrow n_{\mathrm{s,IN}}(T) \quad &= \quad \frac{\sum_{j=1}^{n} N_{\mathrm{i},j}}{\sum_{j=1}^{n} N_{\mathrm{tot},j} \cdot A_j} = \frac{\sum_{j=1}^{n} N_{\mathrm{i},j}}{\sum_{j=1}^{n} A_{\mathrm{tot},j}} = \frac{N_{\mathrm{i}}}{A_{\mathrm{tot}}} && \text{(D5)}
\end{aligned}$$

with $A_{\mathrm{tot},j}$ the total surface area per unit volume of particles in the size bin j and A_{tot} the total surface area over all size bins. ~~In 16 freezing experiments in the AIDA cloud chamber the ice crystal number concentration, formed by active IN, N_{i}, was measured as a function of T. The total particle surface area, A_{tot}, was estimated before each experiment and multiplied with a pressure dilution factor.~~ The evaluation of ~~the results~~ 16 AIDA freezing experiments yields the following fit formula for the ice active surface site density of natural dust:

$$n_{\mathrm{s,IN}}(T)[\mathrm{m}^{-2}] \quad = \quad b \cdot \exp(-A \cdot a \cdot (T - 273.15\ K) + B)\ , \tag{D6}$$

with the fit parameters $A = -0.517$ and $B = 8.934$ and the unit correction factors $a = \mathrm{K}^{-1}$ and $b = \mathrm{m}^{-2}$. Due to the temperature range of the freezing experiments, the parameterization is limited to the ~~temperature range~~ temperatures from 261.15 K to 237.15 K.

Eq. D6 was used here to fit the dataset for the different mineral dust types. The fits were done in two different ways: By using Eq. D3 and Eq. D6 to fit the measured FF (method 1) or by using Eq. D3 to convert the FF measurements to logarithmic surface site densities and fit ~~$n_{\mathrm{s,IN}}(T)$~~ $\ln(n_{\mathrm{s,IN}}(T))$ directly following Eq. D6 (method 2). The results are ~~show~~ shown in Table 6 and in Fig. 11 (method 1). The scheme is labeled "$n_{\mathrm{s,IN}}$" in Fig. 5.

~~Estimated~~

Table 6. Derived fit parameters for the deterministic $n_{\mathrm{s,IN}}$ approach for different mineral dust types. The values are rounded to two digits after the decimal point.

Approach	**Fit ~~parameter~~ parameter**	Kao	Ill	Mont	Micro	ATD
$n_{\mathrm{s,IN}}$ direct	A	~~0.39~~ 0.44	~~0.52~~ 0.37	~~-~~0.34	~~0.17~~ 0.29	~~0.48~~0.28
(complete dataset)	B	~~15.62~~ 12.44	~~11.05~~ 15.18	~~-~~16.98	~~25.77~~ 20.78	~~12.23~~19.14
$n_{\mathrm{s,IN}}$ direct	A	~~0.63~~ 0.56	~~2.35~~ 0.7	~~1.02~~ 0.7	~~0.24~~ 0.52	~~1.15~~0.3
(only FF between 0.1 and 0.9)	B	~~6.27~~ 8.38	~~-56.93~~ 3.69	~~-6.4~~ 4.61	~~24.41~~ 15.16	~~-12.48~~18.43
$n_{\mathrm{s,IN}}$ direct	A	~~0.84~~ 0.63	~~2.72~~ 0.76	~~1.42~~ 0.81	~~0.32~~ 0.65	~~0.85~~0.29
(only FF between 0.2 and 0.8)	B	~~-1~~ 5.95	~~-70.28~~ 1.29	~~-21.24~~ 0.88	~~21.91~~ 11.73	~~-1.13~~18.63
$n_{\mathrm{s,IN}}$ based on FF	A	0.92	1.1	0.91	0.73	0.37
(complete dataset)	B	-3.77	-10.35	-2.71	9.63	16.04
$n_{\mathrm{s,IN}}$ based on FF	A	0.77	1.04	0.9	~~1.41~~ 0.73	0.27
(only FF between 0.1 and 0.9)	B	~~1.12~~ 1.13	-8.3	-2.11	~~8.94~~ 9.49	~~19.2~~19.19
$n_{\mathrm{s,IN}}$ based on FF	A	0.62	0.93	0.88	~~1.41~~ 0.74	0.25
(only FF between 0.2 and 0.8)	B	5.97	~~-4.55~~ -4.54	-1.5	~~8.94~~ 9.29	19.84

Table 6 shows that the results for the fit parameters are very different depending on whether the FF is fitted directly or the active site density $n_{\mathrm{s,IN}}$ ~~directly~~is calculated from the FF and fitted afterwards. That is due to the characteristics of the freezing curve. The very small FF at ~~warm~~ high temperatures and limited FF (to 1) at low temperatures ~~leads~~ lead to a flattening of the $n_{\mathrm{s,IN}}$ curve. Calculating $n_{\mathrm{s,IN}}$ at low temperatures from FF close to 1 gives the number of active sites, which was needed to freeze all droplets. However it could be that more actives sites were present than needed to freeze all droplets. Therefore the tail (low and high FF) of the FF dataset is often left out of the fitting. Here we investigate how the fit results and the freezing curves change depending on the share of the dataset accounted for fitting. We use the complete dataset as a first step and then omit FF data higher than 0.9 and lower than 0.1 and 0.8 and 0.2, respectively. Figure 12 shows this exemplary using ~~the~~ a dataset of kaolinite particles ~~. It can be seen in~~ (d=400 nm, t=10 s). In Fig. 12b it can be seen that the surface site density $n_{\mathrm{s,IN}}$ ~~is quite different depending on how it is estimated. The variation in~~ varies depending on the share of the FF dataset. The implication of the different estimations for $n_{\mathrm{s,IN}}$ ~~depending on~~ is shown in Fig. 12c. The freezing curves from the indirect $n_{\mathrm{s,IN}}$ fit (method 1) are not so different from each other and capture the measurements quite well. The variation

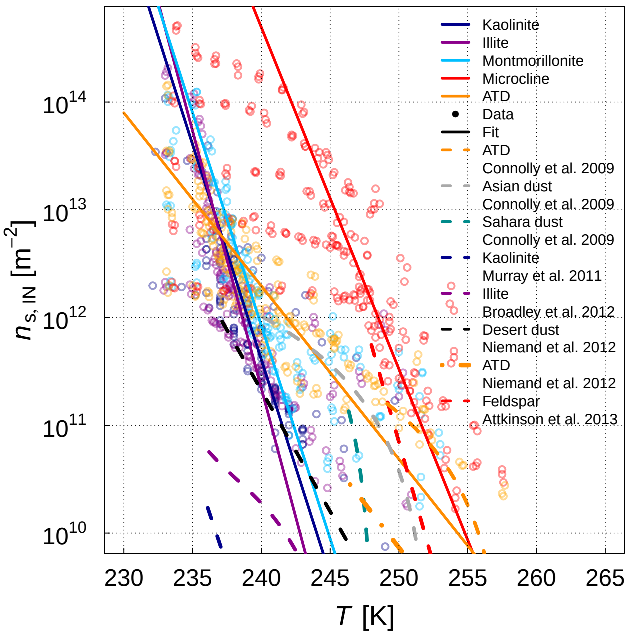

Figure 11. Surface site density $n_{\rm s,IN}$ of different mineral dust types. The points are calculated surface site densities from FF measurements, the lines are the corresponding fits. The fits are based on FF [Eq. D3 and Eq. D6 (method 1); Table 6 (fifth row)]. Some estimates of $n_{\rm s,IN}$ found in literature are added. Colors indicate the dust type, the line type indicates different literature studies.

of the estimated FF due to the share of the FF dataset, which was used for fitting, is larger when $n_{\rm s,IN}$ is estimated directly by fitting ~~to~~ calculated $n_{\rm s,IN}$ from FF measurements (method 2). The largest deviation from all other fits originates when $n_{\rm s,IN}$ is estimated directly taking all data into account. Cutting away the tail of the FF measurements leads to a very similar result when $n_{\rm s,IN}$ is estimated directly (black solid line) compared to the indirect estimate of $n_{\rm s,IN}$ using the complete FF data (red dashed line) ~~. The implication of the different estimations for $n_{\rm s,IN}$ is shown in Fig. 12c for an example dataset of kaolinite (d=400 nm, t=10 s). The freezing curves from the indirect $n_{\rm s,IN}$ fit are not so different from each other and capture the measurements quite well~~[see also Table 6]. When cutting away the tail of the FF data ($FF > 0.2$ and $FF < 0.8$) also the freezing curve based on the direct estimated $n_{\rm s,IN}$ captures the data well and falls on the freezing curve of the indirect $n_{\rm s,IN}$ using the same share of FF data. ~~It seems necessary~~ We recommend to cut the tails ~~away~~ from the FF data when $n_{\rm s,IN}$ is fitted directly. When estimating $n_{\rm s,IN}$ indirectly by using FF ~~it seems that~~ there is no need for cutting the tail. Not cutting the tail increases the amount of data available for the fitting and might therefore be preferable. However, very low/high FF are most susceptible to experimental uncertainties, which could be a legitimation ~~of~~ for cutting the tail away from the dataset. Because the results are different depending on the methodology this sensitivity should be taken into account when comparing different fit parameters of $n_{\rm s,IN}$ from literature. ~~Maybe an uniform standard on how to derive~~ We recommend to estimate $n_{\rm s,IN}$ ~~could help~~indirectly by fitting FF as a standard procedure.

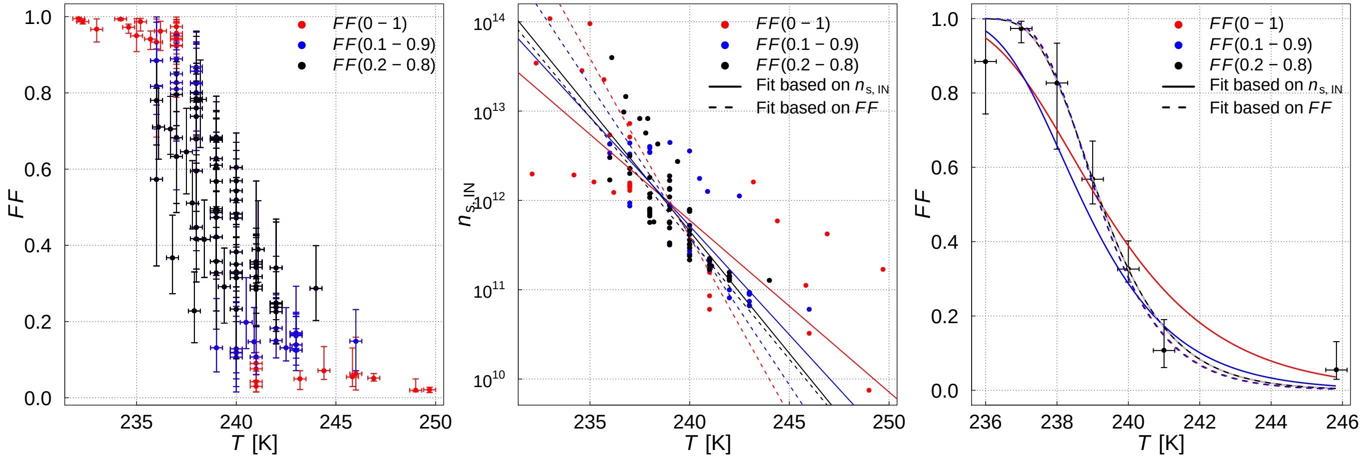

(a) Kaolinite FF dataset.

(b) Calculated $n_{\mathrm{s,IN}}$ based on the FF dataset (points) and fits (lines).

(c) One kaolinite dataset (d=400 nm, t=10 s) with calculated freezing curves using different $n_{\mathrm{s,IN}}$.

Figure 12. Sensitivity study of different methods to estimate the surface site density $n_{\mathrm{s,IN}}$ of kaolinite and ~~its implications~~the resulting freezing curve. The data subsets are color coded as indicated in the legend.

Acknowledgements. The authors would like to thank ~~Corinna Hoose and Paul~~ the anonymous reviewers, P. A. Alpert, C. Hoose and P. Connolly for interesting discussions and their valuable input. Furthermore, we thank S. Ferrachat for the help with estimating the computational costs for extratracers.

References

Alpert, P. A. and Knopf, D. A.: Analysis of isothermal and cooling-rate-dependent immersion freezing by an unifying stochastic ice nucleation model, Atmos. Chem. Phys., 16, 2083–2107, doi:10.5194/acp-16-2083-2016, 2016.

Alpert, P. A., Aller, J. Y., and Knopf, D. A.: Initiation of the ice phase by marine biogenic surfaces in supersaturated gas and supercooled aqueous phases, Phys. Chem. Chem. Phys., 13, 19 882–19 894, doi:10.1039/C1CP21844A, 2011.

Ansmann, A., Tesche, M., Seifert, P., Althausen, D., Engelmann, R., Fruntke, J., Wandinger, U., Mattis, I., and Müller, D.: Evolution of the ice phase in tropical altocumulus: SAMUM lidar observations over Cape Verde, J. Geophys. Res.-Atmos., 114, doi:10.1029/2008JD011659, 2009.

Atkinson, J. D., Murray, B. J., Woodhouse, M. T., Whale, T. F., Baustian, K. J., Carslaw, K. S., Dobbie, S., O'Sullivan, D., and Malkin, T. L.: The importance of feldspar for ice nucleation by mineral dust in mixed-phase clouds, Nature, 498, 355–358, 2013.

Barahona, D.: Thermodynamic derivation of the activation energy for ice nucleation, Atmos. Chem. Phys., 15, 13 819–13 831, doi:10.5194/acp-15-13819-2015, 2015.

Barahona, D., Molod, A., Bacmeister, J., Nenes, A., Gettelman, A., Morrison, H., Phillips, V., and Eichmann, A.: Development of two-moment cloud microphysics for liquid and ice within the NASA Goddard Earth Observing System Model (GEOS-5), Geosci. Model Dev., 7, 1733–1766, 2014.

Broadley, S. L., Murray, B. J., Herbert, R. J., Atkinson, J. D., Dobbie, S., Malkin, T. L., Condliffe, E., and Neve, L.: Immersion mode heterogeneous ice nucleation by an illite rich powder representative of atmospheric mineral dust, Atmos. Chem. Phys., 12, 287–307, doi:10.5194/acp-12-287-2012, 2012.

Cabriolu, R. and Li, T.: Ice nucleation on carbon surface supports the classical theory for heterogeneous nucleation, Phys. Rev. E, 91, 2015.

Chen, J.-P., Hazra, A., and Levin, Z.: Parameterizing ice nucleation rates using contact angle and activation energy derived from laboratory data, Atmos. Chem. Phys., 8, 7431–7449, 2008.

Connolly, P. J., Möhler, O., Field, P. R., Saathoff, H., Burgess, R., Choularton, T., and Gallagher, M.: Studies of heterogeneous freezing by three different desert dust samples, Atmos. Chem. Phys., 9, 2805–2824, doi:10.5194/acp-9-2805-2009, 2009.

Croteau, T., Bertram, A. K., and Patey, G. N.: Observations of high-density ferroelectric ordered water in kaolinite trenches using Monte Carlo simulations, J. Phys. Chem. A, 114, 8396–8405, 2010.

DeMott, P. J., Prenni, A. J., Liu, X., Kreidenweis, S. M., Petters, M. D., Twohy, C. H., Richardson, M. S., Eidhammer, T., and Rogers, D. C.: Predicting global atmospheric ice nuclei distributions and their impacts on climate, Proc. Nati. Acad. Sci. U. S. A., 107, 11 217–11 222, 2010.

Eadie, W. J.: A molecular Theory of the Homogeneous Nucleation of Ice from Supercooled Water, Ph.D. thesis, University of Chicago, 1971.

Edwards, G. R. and Evans, L. F.: Effect of surface charge on ice nucleation by silver iodide, Trans. Faraday Soc., 58, 1649–1655, 1962.

Eidhammer, T., DeMott, P. J., and Kreidenweis, S. M.: A comparison of heterogeneous ice nucleation parameterizations using a parcel model framework, J. Geophys. Res.-Atmos., 114, doi:10.1029/2008JD011095, 2009.

Ervens, B. and Feingold, G.: On the representation of immersion and condensation freezing in cloud models using different nucleation schemes, Atmos. Chem. Phys., 12, 5807–5826, doi:10.5194/acp-12-5807-2012, 2012.

Fletcher, N. H.: Size Effect in Heterogeneous Nucleation, J. Chem. Phys., 29, 572–576, doi:10.1063/1.1744540, 1958.

Hande, L. B., Engler, C., Hoose, C., and Tegen, I.: Seasonal variability of Saharan desert dust and ice nucleating particles over Europe, Atmos. Chem. Phys., 15, 4389–4397, 2015.

Hiranuma, N., Augustin-Bauditz, S., Bingemer, H., Budke, C., Curtius, J., Danielczok, A., Diehl, K., Dreischmeier, K., Ebert, M., Frank, F., Hoffmann, N., Kandler, K., Kiselev, A., Koop, T., Leisner, T., Möhler, O., Nillius, B., Peckhaus, A., Rose, D., Weinbruch, S., Wex, H., Boose, Y., DeMott, P. J., Hader, J. D., Hill, T. C. J., Kanji, Z. A., Kulkarni, G., Levin, E. J. T., McCluskey, C. S., Murakami, M., Murray, B. J., Niedermeier, D., Petters, M. D., O'Sullivan, D., Saito, A., Schill, G. P., Tajiri, T., Tolbert, M. A., Welti, A., Whale, T. F., Wright, T. P., and Yamashita, K.: A comprehensive laboratory study on the immersion freezing behavior of illite NX particles: a comparison of 17 ice nucleation measurement techniques, Atmos. Chem. Phys., 15, 2489–2518, doi:10.5194/acp-15-2489-2015, 2015.

Hoffmann, N., Duft, D., Kiselev, A., and Leisner, T.: Contact freezing efficiency of mineral dust aerosols studied in an electrodynamic balance: quantitative size and temperature dependence for illite particles, Faraday Discuss., 165, 383–390, 2013.

Hoose, C., Kristjánsson, J., Chen, J.-P., and Hazra, A.: A Classical-Theory-Based Parameterization of Heterogeneous Ice Nucleation by Mineral Dust, Soot, and Biological Particles in a Global Climate Model, J. Atmos. Sci., 67, 2010.

Hu, X. L. and Michaelides, A.: Ice formation on kaolinite: Lattice match or amphoterism?, Surf. Sci., 601, 5378–5381, 2007.

Hu, X. L. and Michaelides, A.: Water on the hydroxylated (001) surface of kaolinite: From monomer adsorption to a flat 2D wetting layer, Surf. Sci., 602, 960–974, 2008.

Hurrell, J., Meehl, G. A., Bader, D., Delworth, T. L., Kirtman, B., and Wielicki, B.: A Unified Modeling Approach to Climate System Prediction, Bull. Amer. Meteor. Soc., 90, 1819–1832, doi:10.1175/2009BAMS2752.1, 2009.

Ickes, L., Welti, A., Hoose, C., and Lohmann, U.: Classical nucleation theory of homogeneous freezing of water: thermodynamic and kinetic parameters, Phys. Chem. Chem. Phys., doi:10.1039/C4CP04184D, 2015.

Kanji, Z. A., Welti, A., Chou, C., Stetzer, O., and Lohmann, U.: Laboratory studies of immersion and deposition mode ice nucleation of ozone aged mineral dust particles, Atmos. Chem. Phys., 13, 9097–9118, 2013.

Khvorostyanov, V. I. and Curry, J. A.: A new theory of heterogeneous ice nucleation for application in cloud and climate models, Geophys. Res. Lett., 27, 4081–4084, doi:10.1029/1999GL011211, 2000.

Khvorostyanov, V. I. and Curry, J. A.: The Theory of Ice Nucleation by Heterogeneous Freezing of Deliquescent Mixed CCN. Part I: Critical Radius, Energy, and Nucleation Rate, J. Atmos. Sci., 61, 2676–2691, doi:10.1175/JAS3266.1, 2004.

Khvorostyanov, V. I. and Curry, J. A.: The Theory of Ice Nucleation by Heterogeneous Freezing of Deliquescent Mixed CCN. Part II: Parcel Model Simulation, J. Atmos. Sci., 62, 261–285, doi:10.1175/JAS-3367.1, 2005.

Knopf, D. A. and Forrester, S. M.: Freezing of Water and Aqueous NaCl Droplets Coated by Organic Monolayers as a Function of Surfactant Properties and Water Activity, J. Phys. Chem. A, 115, 5579–5591, doi:10.1021/jp2014644, 2011.

Liu, X., Penner, J. E., Ghan, S. J., and Wang, M.: Inclusion of Ice Microphysics in the NCAR Community Atmospheric Model Version 3 (CAM3), J. Climate, 20, 4526–4547, doi:10.1175/JCLI4264.1, 2007.

Lohmann, U.: A glaciation indirect aerosol effect caused by soot aerosols, Geophys. Res. Lett., 29, 2002.

Lüönd, F., Stetzer, O., Welti, A., and Lohmann, U.: Experimental study on the ice nucleation ability of size-selected kaolinite particles in the immersion mode, J. Geophys. Res.-Atmos., 115, doi:10.1029/2009JD012959, 2010.

Marcolli, C., Gedamke, S., and Zobrist, B.: Efficiency of Immersion Mode Ice Nucleation on Surrogates of Mineral Dust, in: Nucleation and Atmospheric Aerosols, edited by O'Dowd, C. D. and Wagner, P. E., p. 36–40, Springer Netherlands, 2007.

Meyers, M. P., DeMott, P. J., and Cotton, W. R.: New Primary Ice-Nucleation Parameterizations in an Explicit Cloud Model, J. Appl. Meteor., 31, 708–721, doi:10.1175/1520-0450(1992)031<0708:NPINPI>2.0.CO;2, 1992.

Murray, B. J., Broadley, S. L., Wilson, T. W., Atkinson, J. D., and Wills, R. H.: Heterogeneous freezing of water droplets containing kaolinite particles, Atmos. Chem. Phys., 11, 4191–4207, doi:10.5194/acp-11-4191-2011, 2011.

Niedermeier, D., Shaw, R. A., Hartmann, S., Wex, H., Clauss, T., Voigtländer, J., and Stratmann, F.: Heterogeneous ice nucleation: exploring the transition from stochastic to singular freezing behavior, Atmos. Chem. Phys., 11, 8767–8775, doi:10.5194/acp-11-8767-2011, 2011.

Niemand, M., Möhler, O., Vogel, B., Vogel, H., Hoose, C., Connolly, P., Klein, H., Bingemer, H., DeMott, P., Skrotzki, J., and Leisner, T.: A Particle-Surface-Area-Based Parameterization of Immersion Freezing on Desert Dust Particles, J. Atmos. Sci., 69, 3077–3092, doi:10.1175/JAS-D-11-0249.1, 2012.

O'Sullivan, D., Murray, B. J., Malkin, T. L., Whale, T. F., Umo, N. S., Atkinson, J. D., Price, H. C., Baustian, K. J., Browse, J., and Webb, M. E.: Ice nucleation by fertile soil dusts: relative importance of mineral and biogenic components, Atmos. Chem. Phys., 14, 1853–1867, 2014.

Ouchi, K.: Freezing Mechanism of Supercooled Water, Sci. Rep. Tohoku Univ., 6, 43–61, 1954.

Paukert, M. and Hoose, C.: Modeling immersion freezing with aerosol-dependent prognostic ice nuclei in Arctic mixed-phase clouds, J. Geophys. Res.-Atmos., 119, 9073–9092, doi:10.1002/2014JD021917, 2014.

Prenni, A. J., Harrington, J. Y., Tjernström, M., DeMott, P. J., Avramov, A., Long, C. N., Kreidenweis, S. M., Olsson, P. Q., and Verlinde, J.: Can Ice-Nucleating Aerosols Affect Arctic Seasonal Climate?, Bull. Amer. Meteor. Soc., 88, 541–550, 2007.

Pruppacher, H. R. and Klett, J. D.: Microphysics of Clouds and Precipitation, vol. 18, Dordrecht : Kluwer Academic Publishers, 2 edn., doi:10.1007/978-0-306-48100-0, Atmospheric and oceanographic sciences library; 2nd rev. and enl. ed., with an Introduction to cloud chemistry and cloud electricity, 2000.

Reinhardt, A. and Doye, J. P. K.: Note: Homogeneous TIP4P/2005 ice nucleation at low supercooling, J. Chem. Phys., 139, 096102, doi:10.1063/1.4819898, 2013.

Rigg, Y. J., Alpert, P. A., and Knopf, D. A.: Immersion freezing of water and aqueous ammonium sulfate droplets initiated by humic-like substances as a function of water activity, Atmos. Chem. Phys., 13, 6603–6622, 2013.

Šolc, R., Gerzabek, M. H., Lischka, H., and Tunega, D.: Wettability of kaolinite (001) surfaces—Molecular dynamic study, Geoderma, 169, 47–54, 2011.

Storelvmo, T., Hoose, C., and Eriksson, P.: Global modeling of mixed-phase clouds: The albedo and lifetime effects of aerosols, J. Geophys. Res.-Atmos., 116, doi:10.1029/2010JD014724, 2011.

Tobo, Y., DeMott, P. J., Hill, T. C. J., Prenni, A. J., Swoboda-Colberg, N. G., Franc, G. D., and Kreidenweis, S. M.: Organic matter matters for ice nuclei of agricultural soil origin, Atmos. Chem. Phys., 14, 8521–8531, 2014.

Umo, N. S., Murray, B. J., Baeza-Romero, M. T., Jones, J. M., Lea-Langton, A. R., Malkin, T. L., O'Sullivan, D., Neve, L., Plane, J. M. C., and Williams, A.: Ice nucleation by combustion ash particles at conditions relevant to mixed-phase clouds, Atmos. Chem. Phys., 15, 5195–5210, doi:10.5194/acp-15-5195-2015, 2015.

Vali, G.: Nucleation terminology, Bull. Amer. Meteor. Soc., 66, 1426–1427, 1985.

Volmer, M.: Kinetik der Phasenbildung, no. 5 in Die chemische Reaktion, Steinkopff-Verlag, 1939.

Wang, Y., Liu, X., Hoose, C., and Wang, B.: Different contact angle distributions for heterogeneous ice nucleation in the Community Atmospheric Model version 5, Atmos. Chem. Phys., 14, 10 411–10 430, doi:10.5194/acp-14-10411-2014, 2014.

Welti, A., Lüönd, F., Kanji, Z. A., Stetzer, O., and Lohmann, U.: Time dependence of immersion freezing, Atmos. Chem. Phys., 12, 9893–9907, 2012.

Wheeler, M. J., Mason, R. H., Steunenberg, K., Wagstaff, M., Chou, C., and Bertram, A. K.: Immersion Freezing of Supermicron Mineral Dust Particles: Freezing Results, Testing Different Schemes for Describing Ice Nucleation, and Ice Nucleation Active Site Densities, J. Phys. Chem. A, doi:10.1021/jp507875q, 2014.

Wiacek, A., Peter, T., and Lohmann, U.: The potential influence of Asian and African mineral dust on ice, mixed-phase and liquid water clouds, Atmos. Chem. Phys., 10, 8649–8667, doi:10.5194/acp-10-8649-2010, 2010.

Young, K. C.: The role of contact nucleation in ice phase initiation in clouds, J. Atmos. Sci., 31, 768–776, 1974.

Young, T.: An essay on the cohesion of fluids, Philos. Trans. R. Soc., 95, 65–87, 1805.

Zeng, X., Tao, W.-K., Zhang, M., Hou, A. Y., Xie, S., Lang, S., Li, X., Starr, D. O., and Li, X.: A contribution by ice nuclei to global warming, Quart. J. Roy. Meteor. Soc., 135, 1614–1629, 2009.

Zobrist, B., Koop, T., Luo, B. P., Marcolli, C., and Peter, T.: Heterogeneous Ice Nucleation Rate Coefficient of Water Droplets Coated by a Nonadecanol Monolayer, J. Phys. Chem. C, 111, 2149–2155, doi:10.1021/jp066080w, 2007.